Table 1
Average number of phospholipid molecules bound to purified SQR.

The *E. coli* SQR was solubilized using 0.1% (1.9 m*M*), 1.0% (19 m*M*), 2.5% (48 m*M*) and 4.0% (76 m*M*) sucrose monolaurate from membranes with different phospholipid concentrations and purified in the presence of 0.5%(*w*/*v*) Lubrol PX. Values in parentheses are the molar ratios of SML to phospholipid in the membrane suspension.

SML† concentration (m*M*)	Phospholipid concentration in membrane suspension (m*M*)	Average No. of phospholipids per SQR monomer‡§
1.9 (4.8)	0.4	11
19 (0.95)	20	10
19 (4.8)	4.0	8
48 (3.0)	12	6
48 (12)¶	4.0	6
48 (24)	2.0	6
76 (3.8)	20	6
76 (19)	4.0	6

† Sucrose monolaurate (CMC 0.4 m*M*). ‡ The concentration of the purified SQR was estimated by A_{280} (A_{280} = 10.6 for 10 mg ml^{-1} SQR solution). § It was assumed that the phospholipid contained only one P atom. ¶ Crystallization was performed for SQR solubilized under this condition.

530 mg SQR and the pellet obtained by centrifugation was dissolved again in buffer *A*. Residual impurities were successfully removed using a GE Healthcare Source 15Q column (70 ml bed volume). Fractions with an $A_{412}/A_{280} > 0.6$ obtained by elution with 1000 ml of a linear gradient of 0–0.3 *M* NaCl were pooled (Fig. 1, lane 2). The purified SQR (200 mg) was then subjected to sucrose density-gradient ultracentrifugation. The pooled SQR was precipitated by adding solid PEG 3350 and dissolved again in a minimum amount of buffer *A* (~4 ml). The SQR solution (2 ml) was carefully loaded onto buffer *A* (~73 ml) containing a 6–40%(*w*/*v*) sucrose-density gradient and centrifuged at 200 000*g* overnight in a Hitachi P45AT fixed-angle rotor. The SQR, which focused as a deep reddish-coloured sharp band in the middle of the gradient (Fig. 1, lane 3), was separated from the broad pale-reddish upper half in approximately 95% yield, precipitated by PEG 3350 and stored at 193 K for subsequent use. Sodium malonate, an inhibitor of SQR, was added to all of the purification and crystallization steps in order to stabilize the enzyme.

2.5. Detergent exchange

Detergent exchange was performed at 277 K as follows. After purification in the presence of Lubrol PX, the SQR precipitated by PEG 3350 was dissolved in 20 m*M* Tris–HCl buffer pH 7.4 containing 2 m*M* sodium malonate, 200 m*M* KCl and 1% of the detergent of choice. The A_{280} of the SQR solution was set to about 10. After incubation for 20 min on ice, the enzyme was precipitated by adding a 1.4-fold volume of 40%(*w*/*w*) PEG 3350 when the type of detergent exchanged was an *n*-alkyl-oligoethylene glycol monoether (C_nE_m). The pellet obtained by centrifugation was again dissolved in the same buffer and the enzyme was precipitated by PEG 3350 after a 20 min incubation period. This procedure was repeated several times. Exchanges to *n*-alkyl-glucosides (C_nG) and *n*-alkyl-maltosides (C_nM) were performed similarly, but the enzyme was precipitated by adding a 1.2-fold volume of 4.0 *M* ammonium sulfate. Since ammonium sulfate can cause phase separation of a solution containing C_nE_m and PEG can cause phase separation of a solution containing C_nG or C_nM, an appropriate choice of precipitants should be made in order to avoid the denaturation of the enzyme caused by phase separation. The completeness of detergent exchange was checked by thin-layer chromatography (Reiss-Husson, 1992).

Table 2
Average number of phospholipid molecules bound to purified SQR.

The *E. coli* SQR was solubilized and purified using different combinations of detergents. The concentration of phospholipids in the membranes was 4 m*M*, assuming that the phospholipid contained only one P atom.

Detergent used for			
Solubilization (2.5%)	Purification (0.5%)	Average No. of phospholipids per SQR monomer†	Crystallization‡
LDAO§	LDAO	~100	Failed
DOC¶	LDAO	~100	Failed
DOC	SMC††	19	Failed
SMC	SMC	16	Failed
SML‡‡	SML	6	Successful
SML	Lubrol PX§§	6	Successful
Lubrol PX	Lubrol PX	24	Failed
Lubrol PX (4%)	Lubrol PX	6	Successful

† The concentration of the purified SQR was estimated by A_{280} (A_{280} = 10.6 for 10 mg ml^{-1} SQR solution). ‡ Results of crystallization trials according to the optimized procedure described in the text. § *N*,*N*-Dimethyldodecylamine-*N*-oxide (CMC 1.4 m*M*, 0.03%). ¶ Deoxycholic acid (CMC 5 m*M*, 0.2%). †† Sucrose monocaprate (CMC 2.5 m*M*, 0.13%). ‡‡ Sucrose monolaurate (CMC 0.4 m*M*, 0.02%). §§ C_nH_{2n+1}-$(OCH_2CH_2)_m$-OH (n = 12, 14; m = 9.5).

2.6. Crystallization and X-ray diffraction experiments

Crystallization conditions were screened by the hanging-drop vapour-diffusion technique using 96-well CrystalClear Strips (Hampton Research). The SQR was dissolved in 10 m*M* Tris–HCl pH 7.6 buffer containing 2 m*M* sodium malonate and the detergent of choice (A_{280} = 30) and centrifuged for 20 min at 20 000*g* to remove any undissolved material. To set up the hanging-drop vapour diffusion, a droplet made up of 0.5 µl SQR solution and 0.5 µl reservoir solution was incubated over a well containing 100 µl reservoir solution. Initial screening was carried out at 277 and 293 K using the commercially available crystallization kits Crystal Screen (Jancarik & Kim, 1991) and Crystal Screen II from Hampton Research.

X-ray diffraction experiments were performed using the synchrotron beamlines BL44XU at SPring-8 (Harima, Japan), BL-5A at PF and NW12A at PF-AR (Tsukuba, Japan). For X-ray diffraction experiments at 100 K, crystals were transferred to reservoir solution supplemented with 15% glycerol and then frozen by rapid submergence in liquid nitrogen. The data were processed and scaled using programs from the *HKL*-2000 suite (Otwinowski & Minor, 1997).

3. Results and discussion

3.1. Phospholipid content of purified SQR

Since the major constituent (~80% in weight) of the *E. coli* inner membranes is phospholipids (Tanford, 1980), the phospholipid content is a good indicator of the amount of lipid bound to the purified SQR. After solubilization from the membranes using 2.5%(*w*/*v*) sucrose monolaurate and purification in the presence of 0.5%(*w*/*v*) Lubrol PX as described in §2, the concentration of the phosphorus liberated from the phospholipid molecules bound to the purified SQR was measured. Assuming that the phospholipid molecules bound to the purified SQR contained one P atom and that the A_{280} of the 10 mg ml^{-1} SQR solution was 10.6, six bound phospholipid molecules per SQR monomer were detected. The phospholipid contents of SQR prepared under different solubilization conditions were also analyzed. Solubilization with 2.5%(*w*/*v*) or 4.0%(*w*/*v*) sucrose monolaurate gave a value of six regardless of the molar ratio between the detergent and phospholipid in the membrane suspension, whereas the phospholipid content increased to 11 on a decrease in the sucrose monolaurate concentration (Table 1). Therefore, these

six phospholipid molecules seem to be more tightly bound to the SQR. We also performed solubilization and purification using other commercially available detergents (Table 2). *N,N*-Dimethyldodecylamine-*N*-oxide (Fluka) and deoxycholic acid (Wako) produced SQR preparations containing ~100 phospholipid molecules. However, the phospholipid content was reduced to 19 when purification was performed in the presence of 0.5%(*w*/*v*) sucrose monocaprate (Dojindo). Accordingly, most of the phospholipid molecules were loosely bound to the SQR and were removed by the action of 0.5%(*w*/*v*) sucrose monocaprate. On the other hand, 2.5%(*w*/*v*) and 4%(*w*/*v*) Lubrol PX gave phospholipid contents of 24 and six, respectively. In the X-ray structure of *E. coli* SQR solubilized using 4% THESIT, which is virtually the same detergent as Lubrol PX, two well ordered phospholipid molecules, phosphatidylethanolamine and cardiolipin, were found per SQR monomer (Yankovskaya *et al.*, 2003). Since phosphatidylthanolamine and cardiolipin contain one and two P atoms, respectively, there are three P atoms per SQR monomer in the X-ray structure. The disagreement over the number of P atoms probably arises from two causes. Firstly, since the concentration of the SQR was estimated from the calculated molar extinction coefficient in this study, the number of P atoms determined are relative rather than absolute values. Secondly, there may be additional disordered phospholipid molecules which are not detected by X-ray analysis.

Since the Fiske–SubbaRow method only gives an average phospholipid content, it is not known whether or not the purified SQR was uniform in the number of bound phospholipid molecules. Following the Source 15Q column, the purified SQR with six bound phospholipid molecules was subjected to sucrose density-gradient ultracentrifugation at 200 000*g* overnight. After centrifugation, most of the SQR (about 95%) was focused in a sharp deep-reddish band which formed in the middle of the gradient, with a small amount of the enzyme (about 4%) spread broadly at the upper part of the gradient. The phospholipid content of the SQR in the sharp band was six, but in the broad band the phospholipid content was in the range 10–15 depending on the position of the gradient. This result indicates that the uniformity in the phospholipid content was improved by sucrose density-gradient ultracentrifugation.

3.2. Crystallization

After solubilization and purification using 2.5%(*w*/*v*) sucrose monolaurate and 0.5%(*w*/*v*) Lubrol PX, respectively, the purified SQR dissolved in 10 m*M* Tris–HCl buffer pH 7.4 containing 2 m*M* sodium malonate and 0.5%(*w*/*v*) Lubrol PX (50 mg ml^{-1} protein) was subjected to a crystallization trial using commercially available screening kits. Aggregates of small crystals were observed in a large amount of amorphous precipitate using several reservoir solutions containing PEG as a precipitant. An attempt was made to optimize the crystallization conditions by using PEGs with different molecular weights and by varying the PEG concentration, the pH and the temperature. However, none of the conditions investigated improved the results. Since Lubrol PX is a heterogeneous detergent, the detergent was exchanged for commercially available synthetic homogeneous $C_{12}E_8$ and $C_{10}E_8$ (Fluka) and the screening was carried out again. However, no single crystals other than aggregates of small crystals were observed. Additive Screen kits (Hampton Research) were used to examine the effects of adding various compounds but also failed. Single crystals of *E. coli* SQR were finally obtained when either *n*-dodecyl-β-D-maltoside (C_{12}M, Dojindo) or *n*-decyl-β-D-maltoside (C_{10}M, Dojindo) was used as an additive, but their optimum quantities varied subtly from experiment to experiment.

To attain reproducible crystallization, the Lubrol PX in the purified SQR was exchanged for detergent mixtures composed of $C_{12}E_8$ and C_{12}M in ratios of 10:0, 9:1, 8:2 and 7:3 (by weight). Exchange to detergent mixtures with higher C_{12}M content denatured the SQR and the addition of PEG 3350 caused phase separation of the SQR solutions, in which the SQR was concentrated in the phase enriched with the detergent. After detergent exchange, the enzyme was dissolved in 10 m*M* Tris–HCl pH 7.4 and 2 m*M* sodium malonate solution containing $C_{12}E_8$ and C_{12}M in the prescribed ratio with a total concentration of 0.2%(*w*/*v*) and optimization of the crystallization conditions was repeated. Plate-shaped deep-red crystals with typical dimensions of 0.2 × 0.1 × 0.02 mm (Fig. 2*a*) appeared reproducibly within 3 d from reservoir solution composed of 16%(*w*/*v*) PEG 3350, 100 m*M* Tris–HCl pH 8.0, 2 m*M* sodium malonate and 200 m*M* KCl at 293 K when the ratio of $C_{12}E_8$ and C_{12}M was 8:2 (by weight).

Since it has been noted that phase separation plays a major role in the crystallization of membrane proteins (Garavito & Picot, 1990; Reiss-Husson, 1992), the concentrations of PEG 3350 that caused phase separation of solutions containing $C_{12}E_8$ and C_{12}M with a total concentration of 0.2% were examined at 293 K. The 10:0 solution, which contained only 0.2%(*w*/*v*) $C_{12}E_8$ in 100 m*M* Tris–HCl pH 8.0, 2 m*M* sodium malonate and 200 m*M* KCl, separated into two phases at 28%(*w*/*v*) PEG 3350. However, as the ratio of C_{12}M increased, the concentration of PEG 3350 required gradually decreased to 23% and finally to 7%(*w*/*v*) PEG 3350 at 8:2 and 0:10, respectively. Therefore, the crystallization of *E. coli* SQR seems to take place using the 8:2 mixed detergent because the PEG 3350 concentrations necessary for crystallization and phase separation are closer to each other at 8:2 than those observed for the other mixed detergents with lower C_{12}M contents. Interestingly, crystals of the same quality were also obtained at 7.5:2.5, but microcrystals formed only occasionally at 8.5:1.5. Crystals of the same crystal form were also obtained under a similar crystallization condition (20% PEG 3350, 100 m*M* Tris–HCl pH 8.2, 2 m*M* malonate and 200 m*M* KCl at 293 K) using an 8:2 mixture of $C_{12}E_8$ and C_{10}M. X-ray diffraction experiments were performed under liquid-nitrogen-cooled conditions at 100 K using synchrotron radiation. Although fresh crystals diffracted to better than 3 Å resolution, the diffraction limits rapidly reduced to lower than 4 Å resolution owing to radiation damage. Analysis of the symmetry and systematic absences of diffraction patterns indicated that the crystals belonged to the monoclinic space group $P2_1$, with unit-cell para-

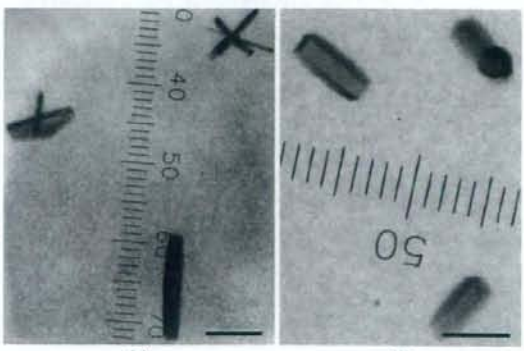

(*a*) (*b*)

Figure 2
Crystals of *E. coli* SQR obtained using (*a*) 0.16% $C_{12}E_8$ and 0.04% C_{12}M and (*b*) 0.16% $C_{10}E_8$ and 0.04% C_{10}M. The scale bar represents 0.2 mm.

Table 3
Statistics of data collection and processing.

Values in parentheses are for the highest resolution shell.

Wavelength (Å)	1.000
Space group	$P4_122$ (or $P4_322$)
Unit-cell parameters	
a (Å)	121.8
b (Å)	121.8
c (Å)	633.4
Solvent content† (%)	62
Resolution range (Å)	40.0–2.9 (3.04–2.9)
No. of reflections	880368
Unique reflections	86980
Completeness (%)	82.0 (85.6)
R_{merge}‡ (%)	8.2 (49.9)
$I/\sigma(I)$	17.1 (3.7)

† Assuming the presence of three molecules in the asymmetric unit. ‡ $R_{merge} = \sum_{hkl}\sum_i |I_i(hkl) - \langle I(hkl)\rangle| / \sum_{hkl}\sum_i I_i(hkl)$.

meters $a = 121.3$, $b = 186.3$, $c = 216.4$ Å, $\beta = 90.6°$. Assuming six SQR molecules (120 kDa × 6) per asymmetric unit, the V_M value (Matthews, 1968) is calculated to be 3.4 Å^3 Da^{-1} with an estimated solvent content of 64%, which is comparable to that found in previous work (69%) by Yankovskaya *et al.* (2003).

In contrast, enzyme for which the detergent was exchanged from Lubrol PX to an 8:2 mixture of $C_{10}E_8$ and either $C_{12}M$ or $C_{10}M$ crystallized in a different crystal form at 293 K from a reservoir solution composed of 20% PEG 3350, 100 m*M* Tris–HCl pH 8.0, 2 m*M* sodium malonate and 200 m*M* KCl (Fig. 2*b*). Diffraction patterns were recorded on the BL44XU beamline of SPring-8 using a DIP6040 detector at a wavelength of 0.9 Å. The crystals belonged to the tetragonal space group $P4_122$ (or $P4_322$), with unit-cell parameters $a = b = 121.8$, $c = 633.4$ Å. Three SQR molecules per asymmetric unit gave a V_M value of 3.3 Å^3 Da^{-1} and an estimated solvent content of 62%. A total of 880 368 observed reflections were merged to 86 980 unique reflections in the 40.0–2.9 Å resolution range. The data-collection and processing statistics are summarized in Table 3. An attempt to solve the structure using the molecular-replacement method with the *MOLREP* program (Navaza, 1994) as implemented in the *CCP*4 package (Collaborative Computational Project, Number 4, 1994) was carried out using the refined coordinates of *E. coli* SQR (PDB code 1nek). A solution with a trimer structure, which was consistent with the previous work of Yankovskaya *et al.* (2003), was obtained in space group $P4_322$. The trimer model was subsequently subjected to rigid-body refinement and gave an R factor of 39%. However, further refinement is not straightforward: the phospholipid molecules were not located currently because the electron densities of the membrane-anchoring hydrophobic regions were faint.

In conclusion, we show that the phospholipid content of purified SQR depends greatly on the detergent used for solubilization and purification and that the enzyme with the fewest bound phospholipid molecules was successfully crystallized in two crystal forms using mixtures of C_nE_m and C_nM. The reaction centre of photosystem II has also been crystallized using detergent mixtures and the role of detergent mixtures in crystallization has been discussed by Rukhman *et al.* (2000). On the basis of the knowledge obtained in this study, we have succeeded in the crystallization of two membrane proteins, quinol:fumarate reductase from *Ascaris suum* mitochondria and recombinant cyanide-insensitive alternative oxidase from *Trypanosoma brucei*, using different mixtures of detergents (details will be published elsewhere).

We are grateful to the staff members at BL44XU at SPring-8 and NW12 and BL-5A at Photon Factory for their help with X-ray diffraction data collection. This work was supported in part by a grant from Japan Aerospace Exploration Agency (JAXA) and by the Targeted Proteins Research Program (TPRP), by Grants-in-Aid for Scientific Research on Priority Areas, for the 21st Century COE Program (F-3), for Creative Scientific Research from the Japanese Ministry of Education, Science, Culture, Sports and Technology (180 73004, 18GS0314, 1903610) and for Scientific Research (B) from Japan Society for the Promotion of Science (18370042). DKI was a research fellow supported by Japan Society for the Promotion of Science.

References

Bartlett, G. R. (1959). *J. Biol. Chem.* **234**, 466–468.
Collaborative Computational Project, Number 4 (1994). *Acta Cryst.* D**50**, 760–763.
Edelhoch, H. (1967). *Biochemistry*, **6**, 1948–1954.
Garavito, R. M. & Picot, D. (1990). *Methods*, **1**, 57–69.
Garavito, R. M. & Rosenbusch, J. P. (1980). *J. Cell Biol.* **86**, 327–329.
Jancarik, J. & Kim, S.-H. (1991). *J. Appl. Cryst.* **24**, 409–411.
Kita, K., Vibat, C. R. T., Meinhardt, S., Guest, J. R. & Gennis, R. B. (1989). *J. Biol. Chem.* **264**, 2672–2677.
Matthews, B. W. (1968). *J. Mol. Biol.* **33**, 491–497.
Michel, H. & Oesterheld, M. (1980). *Proc. Natl Acad. Sci. USA*, **77**, 1283–1285.
Miller, J. H. (1972). *Experiments in Molecular Genetics*. New York: Cold Spring Harbor Laboratory Press.
Navaza, J. (1994). *Acta Cryst.* A**50**, 157–163.
Otwinowski, A. & Minor, W. (1997). *Methods Enzymol.* **276**, 307–326.
Reiss-Husson, F. (1992). *Crystallization of Nucleic Acids and Proteins. A Practical Approach*, edited by A. Ducruix & R. Giegé, p. 176. Oxford University Press.
Rukhman, V., Lerner, N. & Adir, N. (2000). *Photosynth. Res.* **65**, 249–259.
Tanford, C. (1980). *The Hydrophobic Effect*, p. 109. New York: Wiley.
Yamato, I., Anraky, Y. & Hirosawa, K. (1975). *J. Biochem. (Tokyo)*, **77**, 705–718.
Yankovskaya, V., Horsefield, R., Törnroth, S., Luna-Chavez, C., Miyoshi, H., Léger, C., Byrne, B., Cecchini, G. & Iwata, S. (2003). *Science*, **299**, 700–704.

RESEARCH LETTER

Identification of new inhibitors for alternative NADH dehydrogenase (NDH-II)

Tatsushi Mogi[1], Kazunobu Matsushita[2], Yoshiro Murase[3], Kenji Kawahara[1], Hideto Miyoshi[4], Hideaki Ui[5], Kazuro Shiomi[5], Satoshi Ōmura[5] & Kiyoshi Kita[1]

[1]Department of Biomedical Chemistry, Graduate School of Medicine, The University of Tokyo, Tokyo, Japan; [2]Department of Biological Chemistry, Faculty of Agriculture, Yamaguchi University, Yamaguchi, Japan; [3]Mycobacterium Reference Center, The Research Institute of Tuberculosis, Antituberculosis Association, Tokyo, Japan; [4]Division of Applied Life Sciences, Graduate School of Agriculture, Kyoto University, Kyoto, Japan; and [5]Kitasato Institute for Life Sciences and Graduate School of Infection Control Sciences, Kitasato University, Tokyo, Japan

Correspondence: Tatsushi Mogi, Department of Biomedical Chemistry, Graduate School of Medicine, The University of Tokyo, Bunkyo-ku, Tokyo 113-0033, Japan. Tel.: +81 3 5841 8202; fax: +81 3 5841 3444; e-mail: tmogi@m.u-tokyo.ac.jp

Received 7 October 2008; accepted 6 November 2008.
First published online 8 December 2008.

DOI:10.1111/j.1574-6968.2008.01451.x

Editor: Atsushi Yokota

Keywords
acetic acid bacteria; respiratory chain; NADH dehydrogenase; inhibitor; antibiotics.

Abstract

In bacterial membranes and plant, fungus and protist mitochondria, NADH dehydrogenase (NDH-II) serves as an alternative NADH : quinone reductase, a non-proton-pumping single-subunit enzyme bound to the membrane surface. Because NDH-II is absent in mammalian mitochondria, it is a promising target for new antibiotics. However, inhibitors for NDH-II are rare and unspecific. Taking advantage of the simple organization of the respiratory chain in *Gluconobacter oxydans*, we carried out screening of natural compounds and identified scopafungin and gramicidin S as inhibitors for *G. oxydans* NDH-II. Further, we examined their effects on *Mycobacterium smegmatis* and *Plasmodium yoelii* NDH-II as model pathogen enzymes.

Introduction

Obligate aerobe *Gluconobacter* is a genus of acetic acid bacteria that can oxidize a broad range of sugars, sugar alcohols and sugar acids. Low biomass yield and the rapid and incomplete oxidation of carbon sources (oxidative fermentation), which take place in the periplasm and is accompanied by the accumulation of products into the culture medium, make them suitable for industrial applications for bioconversion to obtain a variety of valuable products (Deppenmeier *et al.*, 2002; Adachi *et al.*, 2007). Key oxidation processes are catalyzed by dehydrogenases bound to the outer surface of the cytoplasmic membrane, and linked to the generation of proton-motive force (Matsushita *et al.*, 1994).

The recently released complete genome of *Gluconobacter oxydans* American Type Culture Collection 621H indicates that the respiratory chain lacks Complex I (NADH : quinone reductase, NDH-I), Complex II (succinate : quinone reductase) and Complex IV (cytochrome *c* oxidase) (Prust *et al.*, 2005). Genes encoding putative Complex III (quinol : cytochrome *c* reductase) and cytochrome *c* have been identified, but their functions are unclear because of the absence of cytochrome *c* oxidase. NADH produced in the cytoplasm is reoxidized by a single-subunit NADH dehydrogenase (NDH-II), a key enzyme for the regeneration of an oxidized form of NAD. NDH-II is bound peripherally to the inner surface of the cytoplasmic membrane and does not pump proton. Quinols generated by membrane-bound dehydrogenases are directly oxidized by cytochrome bo_3 oxidase (Matsushita *et al.*, 1987) and/or cyanide-insensitive oxidase (Ameyama *et al.*, 1987).

Taking advantage of the simple organization of the *Gluconobacter* respiratory chain (Matsushita *et al.*, 1994), here, we identified new inhibitors for NDH-II, which has been shown to be crucial for the adaptation of *Mycobacterium tuberculosis* (Shi *et al.*, 2005) and malaria parasite *Plasmodium* spp. (Fisher *et al.*, 2007) to host environments. From the screening of natural antibiotics in the Kitasato Institute for Life Sciences Chemical Library (Ui *et al.*, 2007),

we found the inhibitory activity of 36-membered ring macrolide scopafungin (Johnson & Dietz, 1971) and cyclic decapeptide gramicidin S (GS) (Izumiya *et al.*, 1979) (Fig. 1) for the *G. oxydans* NDH-II, and we examined their inhibitory mechanism and effects on *Mycobacterium smegmatis* and *Plasmodium yoelii* NDH-II.

Materials and methods

Preparation of bacterial membrane vesicles

Gluconobacter oxydans NBRC3172 (formerly *G. suboxydans* IFO12528) was grown aerobically in complex media containing 20 g of sodium D-gluconate, 5 g of D-glucose, 3 g of glycerol, 3 g of yeast extract and 2 g of polypepton (Nihon Pharmaceutical Co.) per 1 L using a 50-L jar fermentor at 30 °C. Cells were harvested at the late-log phase, suspended in 10 mM potassium phosphate (pH 6.0) and disrupted with a Rannie high-pressure laboratory homogenizer (model Mini-Lab, type 8.30H, Wilimington, MA). After centrifugation, to remove intact cells, the supernatant was centrifuged at 86 000 *g* for 60 min and precipitated membranes were suspended in 50 mM Tris-HCl (pH 7.4) containing 10% sucrose and 3 mM EDTA. *Mycobacterium smegmatis* mc^2155 was grown aerobically at 37 °C, and membrane vesicles were prepared from the stationary-phase cells (Kana *et al.*, 2001).

Preparation of malaria parasite mitochondria

Rodent malaria *P. yoelii* strain 17XL was injected intraperitoneally into 8-week-old female BALB/c mice, and parasite mitochondria were prepared as in Takashima *et al.* (2001). Rat liver mitochondria were prepared as in Johnson & Lardy (1967).

Enzyme assay

NADH : ubiquinone-1 (Q_1) reductase (NQR) activity of the membranes was measured at 25 °C in 100 mM Tris-HCl (pH 7.4) containing 10% sucrose, 0.02% Tween 20 (Calbiochem), 10 mM KCN and 100 μM Q_1 with a V-660 double monochromatic spectrophotometer (JASCO, Tokyo, Japan) (Mogi *et al.*, 2008), and reactions were initiated by addition of NADH ($\varepsilon_{340} = 6.3\ mM^{-1}\ cm^{-1}$, Roche) at a final concentration of 200 μM. Mitochondrial NQR and succinate : Q_1 reductase activities were determined in 50 mM potassium phosphate (pH 7.4) containing 1 mM $MgCl_2$, 0.02% Tween 20, 2 mM KCN and 100 μM Q_1 ($\varepsilon_{275} = 12.3\ mM^{-1}\ cm^{-1}$), and reactions were initiated by 200 μM NADH or 10 mM potassium succinate, respectively. NADH oxidase activity was measured in the absence of Q_1. Data analysis was carried out as in Mogi *et al.* (2008).

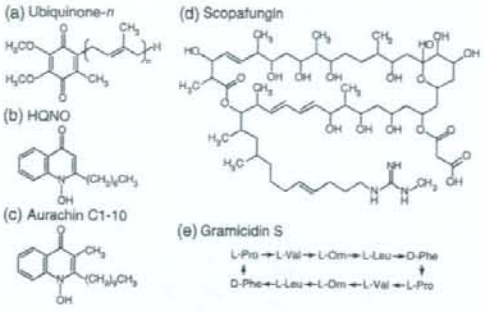

Fig. 1. Structures of ubiquinone, HQNO, aurachin C1–10, scopafungin and GS.

Materials

Synthesis of aurachin C 1-10 (Miyoshi *et al.*, 1999) was carried out as described previously. 2-Heptyl-4-hydroxyquinoline-*N*-oxide (HQNO) was obtained from Sigma.

Results and discussion

Screening of Kitasato Institute for Life Sciences Chemical Library

From the screening of a total of 304 microbial compounds (Ui *et al.*, 2007) at final concentrations of 5 μg mL^{-1} with *G. oxydans* membranes, we revealed the inhibitory activities of scopafungin (niphimycin; residual activity, 33%), GS (31%), polymixin B (51%), aculeacin A (63%), funiculosin (68%) and staurosporine (70%) on 0.2 mM NADH–0.1 mM Q_1 reductase activity of NDH-II.

Inhibitors for NDH-II are rare and mostly unspecific (Kerscher, 2000). Recently, quinolone derivatives [1-hydroxy-2-dodecyl-4(1*H*)quinolone, HQNO and aurachin C] were identified as potent inhibitors for the quinone reduction site of yeast NDH-II (Eschemann *et al.*, 2005; Yamashita *et al.*, 2007). We examined the effects of quinolone inhibitors on the *G. oxydans* NDH-II and found that HQNO and aurachin C 1-10 at 10 μM reduced the NQR activity of the *G. oxydans* membranes to 28% and 12%, respectively, of the control level. Because of the limitation in the availability of isolated natural compounds, we examined further effects of scopafungin and GS (Fig. 1), which are not structurally related to ubiquinone, but showed potent inhibitory activities on the *G. oxydans* NDH-II.

Determination of 50% inhibitory concentration (IC_{50}) values for NDH-II inhibitors

We examined the dependence of the NQR activity on the concentration of GS, scopafungin, HQNO and aurachin C 1-10 and determined their IC_{50} to be 1.2 ± 0.2, 6.2 ± 0.5,

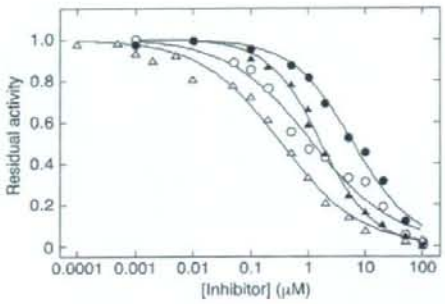

Fig. 2. Inhibition of *Gluconobacter oxydans* NDH-II by scopafungin, GS, HQNO and aurachin C 1-10. NQR activity of *G. oxydans* membranes (10 μg protein mL^{-1}) was determined in the presence of scopafungin (●), GS (○), HQNO (▲) or aurachin C1–10 (△). Data points were average values from duplicate assay. Control activity was 10.2 U mg^{-1} protein. IC_{50} values for GS, scopafungin, HQNO and aurachin C1–10 were estimated to be 1.2, 6.2, 1.7 and 0.34 μM, respectively.

1.7 ± 0.1 and 0.34 ± 0.04 μM, respectively (Fig. 2). The IC_{50} value for GS was < 3.5 μM for the *Escherichia coli bd*-type quinol oxidase (Mogi *et al.*, 2008), and the values for HQNO and aurachin C are comparable to 8 and 0.2 μM, respectively, of yeast *Saccharomyces cerevisiae* NDI1 (Yamashita *et al.*, 2007).

Kinetic analysis of inhibition of NADH-Q_1 reductase activity of NDH-II by scopafungin and GS

NADH-dependent NQR activity showed simple Michaelis–Menten kinetics with an apparent K_m value of 157 μM for NADH (at 0.2 mM Q_1) (Fig. 3). The K_m value for NADH was higher than those reported for yeast *Yarrowia lipolytica* NDE (15 μM) (Kerscher *et al.*, 1999), yeast *S. cerevisiae* NDI1 (31 μM) (de Vries & Grivell, 1988), human malaria *Plasmodium falciparum* NDH-II (17 μM) (Biagini *et al.*, 2006) and *E. coli* Ndh (34 μM) (Björklöf *et al.*, 2000). Q_1-dependent NQR activity followed Michaelis–Menten kinetics with an apparent K_m value of 16.2 ± 0.7 μM (Q_1) (Fig. 4), which is similar to 16 μM (Q_1) in *P. falciparum* (Biagini *et al.*, 2006), 5.9 μM (Q_1) in *E. coli* (Björklöf *et al.*, 2000), 6.4 μM (Q_2) in *M. tuberculosis* (Kana *et al.*, 2001) and 7 μM (decyl benzoquinone) in *Y. lipolytica* (Eschemann *et al.*, 2005).

Macrolide scopafungin and cyclic decapeptide GS (Fig. 1) are structurally unrelated to both NADH and ubiquinone, and serve as noncompetitive inhibitors ($K_i = 5.5$ and 1.4 μM, respectively) for the NADH-binding site of NDH-II (Fig. 3). Unexpectedly, scopafungin and GS were found to be a mixed-type inhibitor and a competitive inhibitor for the quinone-binding site, respectively (Fig. 4). These results

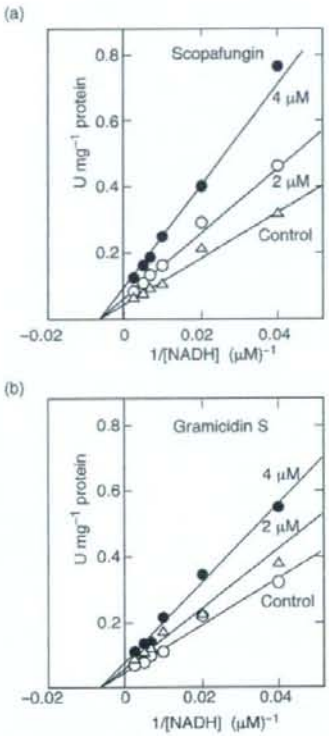

Fig. 3. Kinetic analysis of effects of scopafungin and GS on the NADH-dependent NQR activity of *Gluconobacter oxydans* NDH-II. (a) Noncompetitive inhibition by scopafungin. Apparent V_{max} values were estimated to be 19.3 (control), 17.2 (2 μM scopafungin) and 11.9 (4 μM scopafungin) U mg^{-1} protein at $K_m = 157$ μM. (b) Noncompetitive inhibition by GS. Apparent V_{max} values were determined to be 21.9 (control), 16.5 (2 μM GS) and 13.2 (4 μM GS) U mg^{-1} protein at $K_m = 157$ μM.

indicate that both compounds bind to a hydrophobic binding pocket on NDH-II molecule, which is closer to the quinone reduction site.

Effects of scopafungin and GS on *M. smegmatis* and *P. yoelii* NDH-II

Macrolide antibiotics are known to be more active against Gram-positive bacteria and fungi (Izumiya *et al.*, 1979), but targets remain to be determined while GS is active against Gram-positive and Gram-negative bacteria and several pathogenic fungi (Kondejewski *et al.*, 1996). The primary mode of the action of GS is generally assumed to perturb lipid packing, resulting in the destruction of the membrane integrity and enhancement of the permeability of the lipid bilayer (Prenner *et al.*, 1997). Very recently, we found that

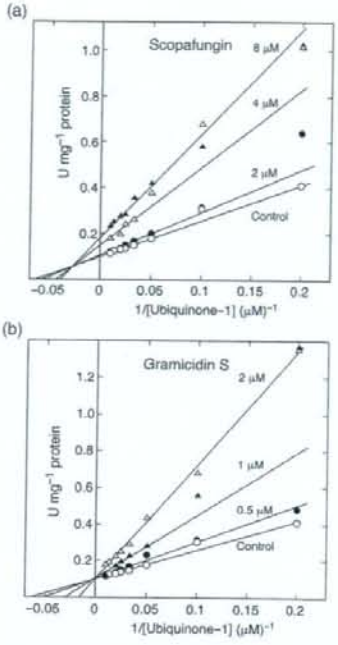

Fig. 4. Kinetic analysis of effects of scopafungin and GS on the Q_1-dependent NQR activity of *Gluconobacter oxydans* NDH-II. (a) Mixed-type inhibition by scopafungin. Apparent K_m (μM) and V_{max} (U mg^{-1} protein) values were estimated to be 15.5 and 9.6 (control), 17.4 and 9.0 (2 μM scopafungin), 22.4 and 6.5 (4 μM scopafungin) and 24.9 and 5.3 (8 μM scopafungin). (b) Competitive inhibition by GS. The apparent K_m values were determined to be 16.9 (control), 21.7 (0.5 μM GS), 37.5 (1 μM GS) and 68.3 (2 μM GS) μM at V_{max} = 10.1 U mg^{-1} protein.

GS can directly inhibit the *E. coli bd*-type quinol oxidase in a mixed-type manner (Mogi *et al.*, 2008). From the screening of the Kitasato Institute for Life Sciences Chemical Library with *G. oxydans* membranes, here, we identified scopafungin and GS as new inhibitors for NDH-II.

NDH-II is a promising target of new antibiotics because of the absence of NDH-II in mammalian mitochondria. The antiplasmodial activities of NDH-II inhibitors, HQNO (IC_{50} = 3.5 μM) (Fry *et al.*, 1990) and 1-hydroxy-2-dodecyl-4(1H) quinolone (IC_{50} = 14 nM) (Saleh *et al.*, 2007), have been reported previously. Thus, we examined the effects of scopafungin and GS on the NQR activity of *M. smegmatis* and rodent malaria *P. yoelii* NDH-II. At 10 μM, scopafungin showed minor effects on rat liver mitochondrial Complex I, Complex II and Complex III *plus* IV, while GS reduced NADH oxidase activity to 35% of the control by inhibiting the Complex III *plus* IV activity (Table 1). Although the IC_{50} values of scopafungin and GS for rodent malaria NDH-II were rather high (16.1 ± 3.0 and 23.0 ± 7.1 μM, respectively), both scopafungin and GS inhibited *M. smegmatis* NDH-II with IC_{50} values of 9.8 ± 0.7 and 2.0 ± 0.1 μM, respectively (Fig. 5), which are better than 12 μM of trifluoperazine for *M. tuberculosis* NDH-II (Yano *et al.*, 2006). Because scopafungin did not show severe effects on mammalian respiratory enzymes, it is a candidate for antimycobacterial agents. Here, we showed that the Kitasato Institute for Life Sciences Chemical Library (Ui *et al.*, 2007) was a powerful source for new potent antibiotics targeting to respiratory enzymes. For the identification of potential candidates, screening with recombinant NDH-IIs is currently underway in our laboratory.

Table 1. Effects of GS and scopafungin on the rat liver mitochondrial respiratory enzymes

	Relative residual activity (%)	
Enzyme activity	10 μM GS	10 μM scopafungin
NADH : Q_1 reductase (Complex I)	107	89
Succinate : Q_1 reductase (Complex II)	90	82
NADH oxidase (Complexes I+III+IV)	35	84

Control activities were 154 (NADH : Q_1 reductase), 247 (succinate : Q_1 reductase) and 102 (NADH oxidase) mU mg^{-1} protein.

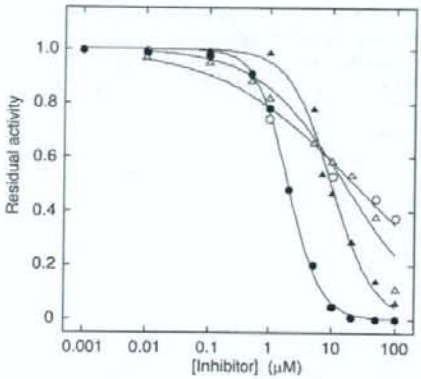

Fig. 5. Inhibition of *Mycobacterium smegmatis* and *Plasmodium yoelii* NDH-II by GS and scopafungin. Control activities of *M. smegmatis* membranes and *P. yoelii* mitochondria were 1.1 and 0.071 U mg^{-1} protein, respectively. The IC_{50} values for GS were estimated to be 2.0 (*M. smegmatis*, ●) and 23 (*P. yoelii*, ○) μM and those for scopafungin were 9.8 (*M. smegmatis*, ▲) and 16 (*P. yoelii*, △) μM.

Acknowledgements

This study was supported by a grant-in-aid for scientific research (20570124 to T.M.), scientific research on Priority Areas (18073004 to K.K.) and Creative Scientific Research (18GS0314 to K.K.) from the Japanese Ministry of Education, Science, Culture, Sports, and Technology.

References

Adachi O, Ano Y, Toyama H & Matsushita K (2007) Biooxidation with PQQ- and FAD-dependent dehydrogenases. *Modern Biooxidation, Enzymes, Reactions and Applications* (Schmid RD & Urlacher VB, eds), pp. 1–41. Wiley-VCH, Weinheim.

Ameyama M, Matsushita K, Shinagawa E & Adachi O (1987) Sugar-oxidizing respiratory chain of *Gluconobacter suboxydans*. Evidence for a branched respiratory chain and characterization of respiratory chain-linked cytochromes. *Agr Biol Chem* **51**: 2943–2950.

Biagini GA, Viriyavejakul P, O'Neill PM, Bray PG & Ward SA (2006) Functional characterization and target validation of alternative Complex I of *Plasmodium falciparum* mitochondria. *Antimicrob Agents Ch* **50**: 1841–1851.

Björklöf K, Zickermann V & Finel M (2000) Purifiction of the 45 kDa, membrane bound NADH dehydrogenase of *Escherichia coli* (NDH-2) and analysis of its interaction with ubiquinone analogs. *FEBS Lett* **467**: 105–110.

Deppenmeier U, Hoffmeister M & Prust C (2002) Biochemistry and biotechnological applications of *Gluconobacter* strains. *Appl Microbiol Biot* **60**: 233–242.

De Vries S & Grivell LA (1988) Purification and characterization of a rotenone-insensitive NADH : Q_6 oxidoreductase from mitochondria of *Saccharomyces cerevisiae*. *Eur J Biochem* **176**: 377–341.

Eschemann A, Galkin A, Oettmeier W, Brandt U & Kerscher S (2005) HDQ (1-hydroxy-2-dodecyl-4(1*H*)quinolone), a high affinity inhibitor for mitochondrial alternative NADH dehydrogenase: evidence for a ping-pong mechanism. *J Biol Chem* **280**: 3138–3142.

Fisher N, Bray PG, Ward SA & Biagini GA (2007) The malaria parasite type II NADH : quinone oxidoreductase: an alternative enzyme for an alternative lifestyle. *Trends Parasitol* **23**: 305–310.

Fry M, Webb E & Pudney M (1990) Effect of mitochondrial inhibitors on adenosine triphosphate levels in *Plasmodium falciparum*. *Comp Biochem Physiol* **B96**: 775–782.

Izumiya N, Kato T, Aoyaga H, Waki M & Kondo M (1979) *Synthetic Aspects of Biologically Active Cyclic Peptides: Gramicidin S and Tyrocidines*. Halsted Press, New York.

Johnson D & Lardy H (1967) Isolation of liver or kidney mitochondria. *Methods in Enzymology, Vol. 10* (Estabrook RW & Pullman ME, eds), pp. 94–96. Academic Press, New York.

Johnson LE & Dietz A (1971) Scopafungin, a crystalline antibiotic produced by *Streptomyces hygroscopicus* var. *enhygrus* var. *nova*. *Appl Microbiol* **22**: 303–308.

Kana BD, Weinstein EA, Avarbock D, Dawes SS, Rubin H & Mizrahi V (2001) Characterization of the *cydAB*-encoded cytochrome *bd* oxidase from *Mycobacterium smegmatis*. *J Bacteriol* **183**: 7076–7086.

Kerscher SJ (2000) Diversity and origin of alternative NADH : ubiquinone oxidoreductase. *Biochim Biophys Acta* **1459**: 274–283.

Kerscher SJ, Okun JG & Brandt U (1999) A single external enzyme confers alternative NADH : ubiquinone oxidoreductase activity in *Yarrowia lipolytica*. *J Cell Sci* **112**: 2347–2354.

Kondejewski LH, Farmer SW, Wishart D, Kay CM, Hancock REW & Hodges RS (1996) Modulation of structure and antibacterial and hemolytic activity by ring size in cyclic gramicidin S analogs. *J Biol Chem* **271**: 25261–25268.

Matsushita K, Shinagawa E, Adachi O & Ameyama M (1987) Purification and characterization of cytochrome *o*-type oxidase from *Gluconobacter suboxydans*. *Biochim Biophys Acta* **894**: 304–312.

Matsushita K, Toyama H & Adachi O (1994) Respiratory chains and bioenergetics of acetic acid bacteria. *Advances in Microbial Physiology, Vol. 36* (Rose AH & Tempest DW, eds), pp. 247–301. Academic Press Ltd, London.

Miyoshi H, Takegami K, Sakamoto K, Mogi T & Iwamura H (1999) Characterization of the ubiquinol oxidation sites in cytochromes *bo* and *bd* from *Escherichia coli* using aurachin C analogues. *J Biochem* **125**: 138–142.

Mogi T, Ui H, Shiomi K, Ōmura S & Kit K (2008) Gramicidin S identified as a potent inhibitor for cytochrome *bd*-type quinol oxidase. *FEBS Lett* **582**: 2299–2302.

Prenner EJ, Lewis RNAH, Newman KC, Gruner SM, Kondejewski LH, Hodges RS & McElhaney RN (1997) Nonlamellar phases induced by the interaction of gramicidin S with lipid bilayers. A possible relationship to membrane disrupting activity. *Biochemistry* **36**: 7906–7916.

Prust C, Hoffmeister M, Liesegang H, Wiezer A, Fricke WF, Ehrenreich A, Gottschalk G & Deppenmeier U (2005) Complete genome sequence of the acetic acid bacterium *Gluconobacter oxydans*. *Nat Biotechnol* **23**: 195–200.

Saleh A, Friesen J, Baumeister S, Gross G & Bohne W (2007) Growth inhibition of *Toxoplasma gondii* and *Plasmodium falciparum* by nanomolar concentrations of 1-hydroxy-2-dodecyl-4(1*H*)quinolone, a high-affinity inhibitor of alternative (type II) NADH dehydrogenases. *Antimicrob Agents Ch* **51**: 1217–1222.

Shi L, Sohaskey CD, Kana BD, Dawes S, North RJ, Mizrahi V & Gennaro ML (2005) Changes in energy metabolism of *Mycobacterium tuberculosis* in mouse lung and under *in vitro* conditions affecting aerobic respiration. *P Natl Acad Sci USA* **102**: 15629–15634.

Takashima E, Takamiya S, Takeo S, Mi-ichia F, Amino H & Kita K (2001) Isolation of mitochondria from *Plasmodium falciparum* showing dihydroorotate dependent respiration. *Parasitol Int* **50**: 273–278.

Ui H, Ishiyama A, Sekiguchi H, Namatame M, Nishihara A, Takahashi A, Shiomi K, Otoguro K & Ōmura S (2007) Selective and potent *in vitro* antimalarial activities found in four microbial metabolites. *J Antibiot* **60**: 220–222.

Yamashita T, Nakamaru-Ogiso E, Miyoshi H, Matsuo-Yagi A & Yagi T (2007) Roles of bound quinone in the single subunit NADH–quinone oxidoreductase (Ndi1) from *Saccharomyces cerevisiae*. *J Biol Chem* **282**: 6012–6020.

Yano T, Li L-S, Weinstein E, The J-S & Rubin H (2006) Steady-state kinetics and inhibitory action of antitubercular phenothiazines on *Mycobacterium tuberculosis* type-II NADH-menaquinone oxidoreductase (NDH-2). *J Biol Chem* **281**: 11456–11463.

J. Biochem. 2009;145(2)229–237
doi:10.1093/jb/mvn161

Mitochondrial Dehydrogenases in the Aerobic Respiratory Chain of the Rodent Malaria Parasite *Plasmodium yoelii yoelii*

Kenji Kawahara[1], Tatsushi Mogi[1,*], Takeshi Q Tanaka[1], Masayuki Hata[1], Hideto Miyoshi[2] and Kiyoshi Kita[1,†]

[1]Department of Biomedical Chemistry, Graduate School of Medicine, the University of Tokyo, Hongo, Bunkyo-ku, Tokyo 113-0033; and [2]Division of Applied Life Sciences, Graduate School of Agriculture, Kyoto University, Sakyo-ku, Kyoto 606-8502, Japan

Received October 7, 2008; accepted November 19, 2008; published online December 6, 2008

In the intraerythrocytic stages of malaria parasites, mitochondria lack obvious cristae and are assumed to derive energy through glycolysis. For understanding of parasite energy metabolism in mammalian hosts, we isolated rodent malaria mitochondria from *Plasmodium yoelii yoelii* grown in mice. As potential targets for antiplasmodial agents, we characterized two respiratory dehydrogenases, succinate:ubiquinone reductase (complex II) and alternative NADH dehydrogenase (NDH-II), which is absent in mammalian mitochondria. We found that *P. y. yoelii* complex II was a four-subunit enzyme and that kinetic properties were similar to those of mammalian enzymes, indicating that the *Plasmodium* complex II is favourable in catalysing the forward reaction of tricarboxylic acid cycle. Notably, *Plasmodium* complex II showed IC_{50} value for atpenin A5 three-order of magnitudes higher than those of mammalian enzymes. Divergence of protist membrane anchor subunits from eukaryotic orthologs likely affects the inhibitor resistance. Kinetic properties and sensitivity to 2-heptyl-4-hydroxyquinoline-*N*-oxide and aurachin C of NADH: ubiquinone reductase activity of *Plasmodium* NDH-II were similar to those of plant and fungus enzymes but it can oxidize NADPH and deamino-NADH. Our findings are consistent with the notion that rodent malaria mitochondria are fully capable of oxidative phosphorylation and that these mitochondrial enzymes are potential targets for new antiplasmodials.

Key words: complex II, inhibitor, mitochondria, NDH-II, rodent malaria.

Abbreviations: AC, aurachin C; DCIP, 2,4-dichlorophenolindophenol; DHO, dihydroorotate; DHOD, DHO dehydrogenase; HQNO, 2-heptyl-4-hydroxyquinoline-*N*-oxide; hrCNE, high-resolution clear-native electrophoresis; IC_{50}, the 50% inhibitory concentration; NBT, nitro blue tetrazolium chloride; NDE, NDH-II bound to the outer surface of the mitochondrial inner membrane; NDI, NDH-II bound to the matrix side of the mitochondrial inner membrane; NQR, NADH:quinone reductase; Q_n, ubiquinone-n; SDH, succinate dehydrogenase; SQR, succinate:quinone reductase; TCA, tricarboxylic acid.

INTRODUCTION

Malaria remains one of the main global health problems, causing more than 1 million deaths per year, with about 90% of deaths and 60% of cases occurring in Africa, south of the Sahara (*1*). Mortality associated with malaria is mainly caused by the erythrocytic stage cells of human malaria *Plasmodium falciparum*. The emerging resistance against established drugs in *Plasmodium* populations (*2*) emphasizes the urgent need for the development of new antiplasmodial drugs.

Energy metabolism of *Plasmodium* is quite different from that of mammalian hosts. Intraerythrocytic stages of parasites have been considered for a long time to rely on incomplete oxidation of glucose with secretion of end products such as lactate and pyruvate (*3*) and to possess mitochondria that lack oxidative phosphorylation and a functional tricarboxylic acid (TCA) cycle (*4*, *5*). *Plasmodium* spp. lacks genes coded for the proton-translocating NADH dehydrogenase (NDH-I, complex I) present in mammalian mitochondria (*6*, *7*) and uses a rotenone-insensitive single-subunit NADH dehydrogenase (NDH-II) (*8*), which is assumed not to oxidize deamino-NADH (*9*). Succinate:ubiquinone oxidoreductase (complex II, succinate dehydrogenase (SDH)) is a membrane-bound TCA cycle enzyme and consists of four subunits: a flavoprotein subunit (Fp, SDH1) and an iron–sulphur subunit (Ip, SDH2) form a soluble heterodimer, which binds to a membrane anchor *b*-type cytochrome [CybL (SDH3)/CybS (SDH4) heterodimer]. The *Plasmodium SDH1* and *SDH2* genes have been cloned by homology probing (*10*) while SDH3 and SDH4 appear highly divergent from orthologs and are still not annotated in the current database (*6*, *7*). Membrane bound subuniuts *a* and *b* of ATP synthase also remain unidentified (*6*, *7*), and thus complete mitochondrial ATP synthase was assumed to be absent in *Plasmodium* spp. (*4*, *5*, *11–13*). Recently, Painter *et al.* (*13*) claimed that

*To whom correspondence addressed. Tel: +81-3-5841-3526, Fax: +81-3-5841-3444, E-mail: tmogi@m.u-tokyo.ac.jp
†Correspondence may also be addressed. Tel: +81-3-5841-3526, Fax: +81-3-5841-3444, E-mail: kitak@m.u-tokyo.ac.jp

the mitochondrial respiratory chain is required only for the regeneration of an oxidized form of ubiquinone, which serves as the electron acceptor for type 2 dihydroorotate dehydrogenase (DHOD), an essential enzyme for pyrimidine biosynthesis. It is widely accepted that the majority of the parasite's ATP demand is met through glycolysis (*11*).

On the contrary, atovaquone, an inhibitor for ubiquinol:cytochrome *c* reductase (complex III) (*14*), showed the antiplasmodial activity for *P. falciparum* with the 50% inhibitory concentration (IC_{50}) of 1 nM (*15*) and collapsed the mitochondrial membrane potential in *P. yoelii yoelii* (*16*). Uyemura *et al.* (*8*, *17*) demonstrated oxidative phosphorylation and succinate respiration in trophozoites of rodent malaria parasites. These observations suggest that *Plasmodium* mitochondria possess all subunits for canonical complex II and ATP synthase and are fully capable of oxidative phosphorylation.

It was shown recently that metabolism in *P. falciparum* parasites grown in human patients is affected by varied oxygen and substrate levels and by host-parasite interactions (*18*). The authors found the induction of gene sets associated with oxidative phosphorylation including respiratory enzymes. For understanding energy metabolism in malaria parasites, the isolation of active mitochondria from parasites, which have been adapted to host environments, is essential. In this study, *P. y. yoelii* mitochondria were isolated from parasites grown in mouse erythrocytes and enzymatic properties of complex II and NDH-II were characterized. Two-dimensional PAGE analysis supports the presence of membrane anchors in *Plasmodium* complex II. These findings indicate that *Plasmodium* mitochondria are fully capable of succinate-dependent oxidative phosphorylation as suggested by previous observations (*8*, *17*). Because the difference in the inhibitor sensitivity of complex II between *Plsamodium* and mammalian enzymes and the absence of NDH-II in mammalian mitochondria, these two enzymes are promising targets for new antimaralials.

MATERIALS AND METHODS

Parasite Culture—Animal care and experimental procedures were performed according to the Guidelines for Animal Experimentation, the University of Tokyo. *P. y. yoelii* strain 17XL was a kind gift of H. Otsuki (Ehime University). This strain can rapidly propagate without cerebral malaria and does not infect reticulocytes. About 3.0×10^7 parasites were injected intraperitoneally to 8-week-old female BALB/c mice, and the developmental stage and parasitemia were monitored by examination of Giemsa-stained thin blood smears. About 7.5 ml of the blood was collected from 10 mice by cardiac puncture 130–140 h after infection. To remove leukocytes and platelets, the blood was mixed with 0.5 ml of heparine and passed over a powdered cellulose column (CF11; Whatman, Clifton; 0.5 ml/ml blood), which has been equilibrated with 20 ml of PBS (*19*). Erythrocytes were eluted with 30 ml of PBS and collected by centrifugation at 4°C at $800 \times g$ for 5 min. In control experiments with uninfected mice, microscopic observations and examination of complex II and dihydroorotate dehydrogenase (DHOD) activities excluded the possible contamination of mouse leukocytes in the eluate. Erythrocytes were washed three times with RPMI-1640 medium (Gibco) and then transferred to RPMI-1640 medium supplemented with 10% AlbuMax I (Gibco) at the hematoclit of 3%. Then erythrocytes were incubated at 37°C for 2 h under conditions of 90% N_2, 5% O_2 and 5% CO_2, and trophozoite-rich parasites were recovered by centrifugation as above.

Preparation of Mitochondria—To isolate parasites, infected erythrocytes were lysed for 10 min on ice with 0.1% (w/v) saponin and the lysate was centrifuged at 4°C at $2,380 \times g$ for 10 min to remove erythrocyte membranes. Parasites were washed twice with PBS by centrifugation at 4°C at $5,800 \times g$ for 10 min and resuspended with 10–20 ml of buffer A [225 mM mannitol, 75 mM sucrose, 5 mM $MgCl_2$, 5 mM KH_2PO_4, 5 mM HEPES, 1 mM EGTA (pH 7.4)], supplemented with 0.1% (w/v) fatty acid-free bovine serum albumin (PAA Cell Culture Co.), 1 mM phenylmethanesufonyl fluoride (Sigma) and 1 × Protease Inhibitor Cocktail for general use (Sigma). Parasites were disrupted by N_2 cavitation at 1,200 psi for 20 min with 4639 Cell Disruption Bomb (Parr, USA) (*20*). Lysate was centrifuge at 4°C at $700 \times g$ for 8 min, and the resultant precipitate containing unbroken parasites was resuspended with 10 ml of buffer A and disrupted as above. This procedure was repeated twice to improve the parasite yield. Crude mitochondria were recovered from the supernatant by centrifugation at 4°C at $10,000 \times g$ for 8 min and suspended in buffer A at ~5 mg protein/ml. Rat liver mitochondria were prepared as described by Johnson and Lardy (*21*).

Enzyme Assay—Enzyme assay was performed at 25°C with V-660 double monochromatic spectrophotometer (JASCO, Tokyo, Japan; <0.00005 Abs noise) or UV-3000 double wavelength spectrophotometer (Shimadzu Corp., Kyoto, Japan), and reactions were started by addition of substrates (electron donors). Succinate:quinone reductase (SQR) activity was determined as quinone-mediated succinate:2,4-dichlorophenolindophenol (DCIP) reductase in 50 mM potassium phosphate (pH 8.0) containing 10 mM potassium succinate, 100 μM ubiquinone-2 (Q_2) and 45 μM DCIP ($\varepsilon_{600} = 21\ mM^{-1}\ cm^{-1}$) in the presence of 2 mM KCN. NADH:ubiquinone reductase (NQR) activity was measured in 50 mM potassium phosphate (pH 8.0) containing 200 μM NADH ($\varepsilon_{340} = 6.22\ mM^{-1}\ cm^{-1}$) and 100 μM ubiquinone-1 (Q_1) in the presence of 10 μM atovaquone and 2 mM KCN (*15*). DHOD activity was measured as DHO:DCIP reductase in 30 mM Tris–HCl (pH 8.0) containing 500 μM DHO, 100 μM Q_2 and 45 μM DCIP in the presence of 2 mM KCN (*20*). DHO:cytochrome *c* reductase activity was determined with 20 μM horse cytochrome *c* ($\varepsilon_{550} = 19\ mM^{-1}\ cm^{-1}$) in place of 45 μM DCIP (*20*). For inhibition studies, the reaction mixture was preincubated for 5 min in the presence of 0.1% (w/v) sucrose monolaurate (Mitsubishi-Kagaku Foods Co., Tokyo, Japan) to disperse hydrophobic substrates and inhibitors. Kinetic analysis and the estimation of the 50% inhibitory concentration (IC_{50}) were performed as described previously (*22*).

Clear-Native Electrophoresis and Activity Staining—Mitochondria were precipitated at 4°C at 20,400 × *g* for 5 min and resuspended at 6 mg protein/ml in 10 mM Tris–HCl (pH 7.4) containing 1% sucrose monolaurate, 1 mM sodium malonate and Protease Inhibitor Cocktail by brief sonication. After 20 min incubation at 4°C with rotating, the mixture was centrifuged at 4°C at 107,000 × *g* for 30 min and supernatant was concentrated at 4°C at 4,000 × *g* with Nanosep ultrafiltration devices (MWCO 100,000, Pall Life Science). Solubilized mitochondrial proteins were subjected to high resolution clear-native electrophoresis (hrCNE) (*23*) with 3–12% Novex gels (Invitrogen) using 0.02% dodecylmaltoside and 0.05% sodium deoxycholate for the cathode buffer additives. Gels were incubated at 25°C for 10 min in 30 mM Tris–HCl (pH 7.4) containing 20 mM potassium succinate and 0.5 mM nitro blue tetrazolium chloride (NBT), and then complex II band was visualized by 1 h incubation in dark in the presence of 0.2 mg/ml phenazine methosulphate. Protein bands were stained with GelCode (Pierce).

Analysis of Membrane Anchor Subunits of Complex II—Complex II bands identified as succinate:NBT reductase in hrCNE were cut out from gels and equilibrated with an equal amount of 2× SDS–PAGE sample buffer. Gel pieces were applied to 10–20% Supersep gels (Wako Pure Chemicals, Tokyo, Japan) and SDS–PAGE analysis was carried out. Protein bands were visualized by silver staining.

Miscellaneous—Protein contents of mitochondria and solubilized membrane proteins were determined with BIO-RAD and BCA protein assay reagent (Pierce), respectively, using bovine serum albumin as standard. Western blot analysis was carried out using anti-*P. falcifaum* (Pf) Fp and anti-PfIp rabbit antiserum and cross-reacted bands were visualized by alkaline phosphatase-conjugated anti-rabbit IgG (Bio-Rad) (*24*).

RESULTS

Preparation of Plasmodium Mitochondria—After infection of mice with rodent malaria parasites, we monitored amounts of erythrocytes and parasitemia and found that the number of parasites decreased sharply 140 h after infection as the number of the erythrocyte decreased. Thus, we collected the infected blood 130 to 140 h after infection. Leukocyte-free washed erythrocytes were incubated at 37°C for 2 h in RPMI-1640 medium supplemented with 10% AlbuMax I to adjust the developmental stage to trophozoites (trophozoite : ring : schizont = 7 : 2 : 1). Then the parasites were released from infected erythrocytes with 0.1% saponin and disrupted by the N_2 cavitation method (*20*).

Yield of Plasmodium Mitochondria—SQR activity and DHOD activity of *P. y. yoelii* mitochondria were 5- and 3-fold, respectively, higher than those of the axenic cultured *P. falciparum* (*20*). Furthermore, yields of mitochondrial proteins (5.5 ± 1.3 mg protein) and total activities of complex II (56 ± 14 mU) and DHOD (132 ± 18 mU) after preparation from ten infected mice were much greater than those of *P. falciparum* mitochondria [1 mg protein, 2 mU (*25*), and 7 mU (*20*), respectively, from the 360-ml *in vitro* culture]. Thus, in terms of the yield and specific activity, *P. y. yoelii* mitochondria are suitable for biochemical studies on mitochondrial enzymes of malaria parasites.

Table 1. **Enzymatic properties of *P. y. yoelii* mitochondria.**

Enzyme	Specific activity (mU/mg protein)	
	P. y. yoelii[a]	Rat liver
Succinate:DCIP reductase (complex II)	2.66 ± 0.02	188
NADH:Q_1 reductase[b]	42.2 ± 0.3	152
NADH:Cyt *c* reductase[c]	18.6 ± 1.6	ND[d]
DHO:DCIP reductase (DHOD)	10.5 ± 1.3	2.6
Q_1H_2 oxidase (complex III + complex IV)	19.4 ± 0.2	166

[a]Values were mean ± SD. Freshly prepared *P. y. yoelii* mitochondria showed SQR, NQR and DHOD activities of 10.2 ± 0.1, 63.2 ± 10.1 and 24.1 ± 3.9 mU/mg protein (n = 6), respectively. Enzyme activities were reduced to about one half after freeze-thaw of mitochondria preparations, which have been stored at −80°C. [b]NDH-II of *P. y. yoelii* or NDH-I of rat liver mitochondria were analysed. [c](NDH-II of *P. y. yoelii* or NDH-I of rat liver mitochondria) + complex III were analysed. [d]ND, not determined.

Comparison of Mitochondrial Enzymes from P. y. yoelii and Rat Liver—When comparing with rat liver mitochondria, SQR (complex II), NQR (NDH-II) and Q_1H_2 oxidase (complex III *plus* complex IV) activity of *P. y. yoelii* mitochondria were 1.4%, 28% and 12%, respectively, of rat liver mitochondria whereas DHOD activity was 4-fold higher than that of rat liver mitochondria (Table 1). Rotenone [IC_{50} = 13 nM for bovine complex I (*26*)] inhibited rat liver mitochondria complex I 95–97% at 1 μM while the inhibition of the *P. y. yoelli* NQR activity by 10 μM rotenone was only 20%. Since NQR activity of *P. y. yoelii* mitochondria followed a simple Michaelis–Menten kinetics (see below), we concluded that the enzyme activities are not due to contaminated mouse mitochondria derived from leukocytes or platelets.

Enzymatic Properties of Plasmodium Complex II—SQR activity of *P. y. yoelii* mitochondria displayed Michaelis–Menten kinetics (Fig. 1). Apparent K_m values for succinate and Q_2 were estimated to be 49 and 0.17 μM, respectively, which are close to 20 and 0.5 μM, respectively, of bovine complex II (*27*). Apparent K_m value for Q_1 was found to be 1.6 μM. Differences in K_m value (9-fold) and V_{max}/K_m ratio (19-fold) between Q_1 and Q_2 indicate that the 6-polyprenyl tail of the ubiquinone ring contributes to the binding affinity and that Q_2 is better substrate than Q_1.

Then effects of the quinone-binding site inhibitors on the SQR activity were examined. Atpenin A5 and carboxin are known inhibitors for bovine complex II with IC_{50} values of 4 nM and 1 μM, respectively (*28*) and plumbagin (5-hydroxy-2-methyl-1,4-naphthoquinone) has been reported to inhibit *P. falciparum* complex II (IC_{50} = 5 μM) and the growth (IC_{50} = 0.27 μM) (*29*). At 100 μM Q_2, we found that IC_{50} values for atpenin A5 and carboxin were 4.6 and 3.6 μM, respectively, in *P. y. yoelii* mitochondria and 7.1 nM and 3.8 μM, respectively, in rat liver mitochondria (Fig. 2). The inhibition by plumbagin was only 50% even at 100 μM.

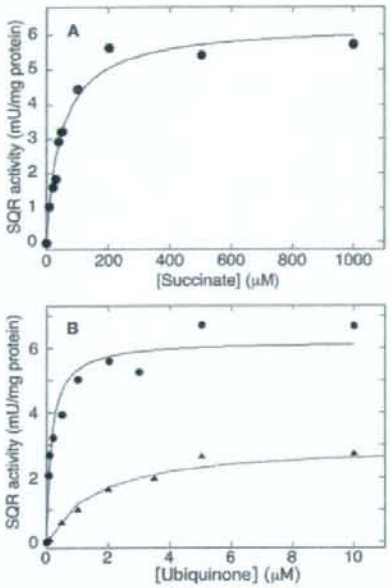

Fig. 1. **Kinetic analysis of SQR activity of *P. y. yoelii* mitochondria.** (A) As a function of the succinate concentration, SQR activity was examined at 6 μg mitochondrial protein/ml in the presence of 0.1 mM Q_2. Data points were averages from three independent preparations (6.19 ± 0.93 mU/mg protein with 1 mM succinate and 0.1 mM Q_2). Data were fitted to Michaelis–Menten kinetics with apparent K_m and V_{max} values of 49.3 ± 7.0 μM and 6.26 ± 0.27 mU/mg protein, respectively. (B) As a function of the Q_1 (circles) or Q_2 (triangles) concentration, SQR activity was examined in the presence of 10 mM succinate. Data points were averages from two independent preparations (6.25 ± 0.87 mU/mg protein with 1 mM succinate and 0.1 mM Q_2). Data were fitted to Michaelis–Menten kinetics with apparent K_m and V_{max} values of 1.61 ± 0.20 μM and 3.03 ± 0.12 mU/mg protein, respectively, for Q_1 and 0.17 ± 0.04 μM and 6.20 ± 0.30 mU/mg protein, respectively, for Q_2.

Membrane Anchor Subunits of Plasmodium Complex II—For reduction of ubiquinone, *Plasmodium* complex II should have a quinone-binding pocket provided by Ip and the CybL/CybS heterodimer (*30–32*). For the examination of subunit structure of *Plasmodium* complex II, we first determined the molecular weight of *P. y. yoelii* complex II by hrCNE, followed by in-gel activity staining as phenazine methosulphate-mediated succinate : NBT reductase. An apparent molecular weight of *P. y. yoelii* complex II was estimated to be 135 kDa (Fig. 3, lane 2), which is comparable to 130 kDa of bovine and yeast complex II (*33*). Western blot analysis identified Fp and Ip as the 70- and 35-kDa proteins, respectively (Fig. 3, lanes 3 and 4), indicating that a sum of molecular weights of membrane anchor subunits is about 30 kDa. Subsequently, the 135-kDa bands in hrCNE were excised from gels and subjected to SDS–PAGE analysis. Due to an extremely low activity of *Plasmodium* complex II (~1% of mammalian mitochondria) and the diffusion of

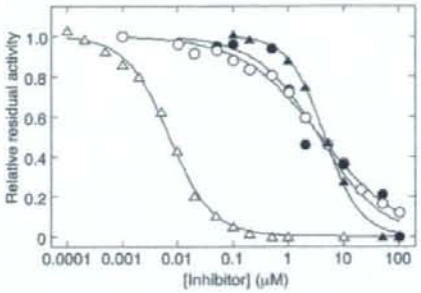

Fig. 2. **Inhibition of SQR activity of *P. y. yoelii* mitochondria by atpenin A5 and carboxin.** SQR activity of *P. y. yoelii* (closed symbols) and rat liver (open symbols) mitochondria was determined with 10 mM potassium succinate and 0.1 mM Q_2 in the presence of atpenin A5 (triangles), and carboxin (circles). Data points were average values from two independent preparations. IC_{50} values were determined to be 4.6 ± 0.2 μM for atpenin A5 and 3.6 ± 1.0 μM for carboxin in *P. y. yoelii* mitochondria and 7.1 ± 0.3 nM for atpenin A5 and 3.8 ± 0.1 μM for carboxin in rat liver mitochondria. Control activitiy of *P. y. yoelii* mitochondria was 2.68 ± 0.03 mU/mg protein.

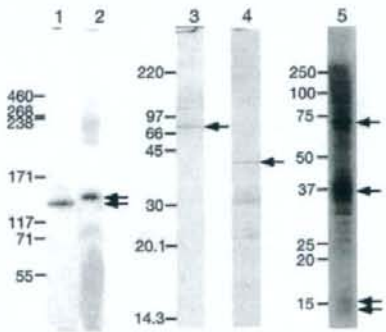

Fig. 3. **Electrophoresis analysis of complex II in *P. y. yoelii* mitochondria.** Solubilized mitochondrial proteins were subjected to hrCNE, and complex II of bovine (lane 1, 2.4 μg protein) and *P. y. yoelii* (lane 2, ~0.4 mg protein) mitochondria were visualized by SDH activity staining. Arrows indicate complex II bands. For Western blot analysis, 10 μg of mitochondrial proteins were subjected to 15% SDS–PAGE and Fp (lane 3) and Ip (lane 4), indicated by arrows, were identified by anti-PfFp and anti-PfIp rabbit antisera, respectively. For identification of *P. y. yoelii* complex II subunits, complex II bands in hrCNE were excised from gels and subjected to 10–20% SDS–PAGE, followed by silver staining (lane 5). Putative subunits of *P. y. yoelii* complex II are indicated by arrows. HiMark Prestained High Molecular Weight Protein Standard (Invitrogen), Rainbow Colored Protein Molecular Weight Marker (High molecular weight range) (Amersham Pharmacia Biotech), and Precision Plus Protein Standard (Bio-Rad) were used as molecular weight standards for lanes 1 and 2, lanes 3 and 4, and lane 5, respectively.

a reduced product of NBT, it was difficult to cut out the complex II band but we were able to identify 70, 35, 16 and 14 kDa bands as putative subunits of the 135-kDa complex (Fig. 3, lane 5).

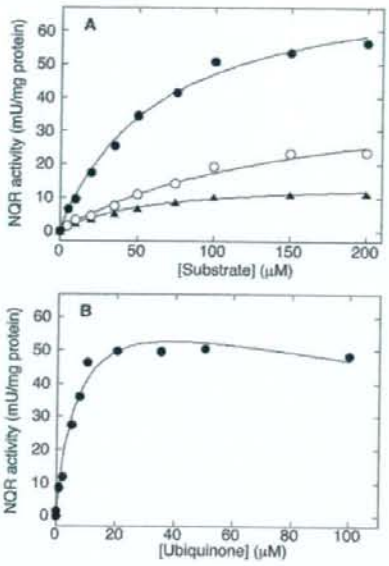

Fig. 4. **Kinetic analysis of NQR activity in *P. y. yoelii* mitochondria.** (A) As a function of the concentration of NADH (closed circle), NADPH (open circle) or deamino-NADH (closed triangle), NQR activity was examined at 6 μg protein/ml in the presence of 0.1 mM Q_1. Data points were averages from two independent preparations (44.9 ± 4.8 mU/mg protein with 0.2 mM NADH). Data were fitted to Michaelis–Menten kinetics with apparent K_m and V_{max} values of 63.2 ± 6.9 μM and 76.7 ± 3.4 mU/mg protein, respectively, for NADH, 157 ± 33 μM and 44.4 ± 5.4 mU/mg protein, respectively, for NADPH, 58.4 ± 5.7 μM and 15.1 ± 0.6 mU/mg protein, respectively, for deamino-NADH. (B) As a function of the concentration of Q_1, NQR activity was examined in the presence of 0.2 mM NADH. Data points were average values from two independent preparations [48.6 ± 7.9 mU/mg protein at 0.1 mM Q_1). Data were fitted to substrate inhibition kinetics with apparent K_m, V_{max} and K_{is} values of 7.2 ± 1.7 μM, 71.8 ± 7.6 mU/mg protein, and 218 ± 97 μM, respectively, using the equation $v = V_{max} S/(K_m + S + S (1+S/K_{is}))$.

Enzymatic Properties of Plasmodium NDH-II—*Plasmodium* spp. lacks genes encoding complex I (*6*, *7*) and uses a single-subunit NADH dehydrogenase (NDH-II) (*8*, *15*). Upon permealization of mitochondria with 30 μg/ml alamethicin, which forms pores large enough to permit the rapid diffusion of NADH (*34*), NQR and SQR activities increased 32% and 27%, respectively, indicating that *Plasmodium* NDH-II is likely located at the matrix side of the inner membrane.

When reactions were started by addition of NADH, NQR activity showed a simple Michaelis–Menten kinetics with apparent K_m and V_{max} values of 63 μM for NADH and 77 mU/mg protein, respectively (Fig. 4A). K_m value for NADH was closer to 31 μM of *Saccharomyces cerevisiae* internal NDH-II (NDI1) (*35*) and 34 μM of *E. coli* NDH-II (*36*) than 15 μM of yeast *Yarrowia lipolytica* external NDH-II (NDE) (*37*). In contrast,

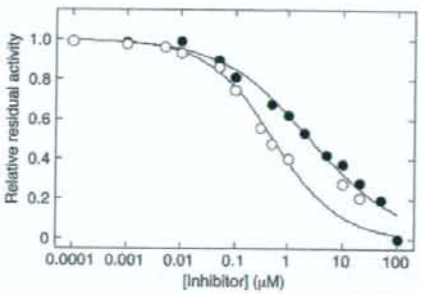

Fig. 5. **Inhibition of NQR activity of *P. y. yoelii* mitochondria by HQNO and Aurachin C1-10.** NQR activity of *P. y. yoelii* mitochondria was determined with 0.2 mM NADH and 0.1 mM Q_1 in the presence of HQNO (closed circle) or aurachin C1-10 (open circle). Data points were average values from two independent preparations. Control activity of *P. y. yoelii* mitochondria was 45.6 ± 1.3 mU/mg protein with 0.1 mM Q_1. IC_{50} values for HQNO and aurachin C1-10 were estimated to be 2.5 ± 0.4 and 0.47 ± 0.03 μM, respectively.

Q_1-started NQR activity showed substrate inhibition kinetics with K_m and K_{is} values of 7 and 218 μM, respectively, for Q_1 (Fig. 4B). Unlike *E. coli* NADH-II (*36*) and *Y. lipolytica* NDE (*37*), *P. y. yoelii* NDH-II can oxidize deamino-NADH (K_m = 58 μM, V_{max} = 15 U/mg protein) and NADPH (K_m = 157 μM, V_{max} = 44 mU/mg protein) (Fig. 5A). V_{max}/K_m ratios indicate that *Plasmodium* NDH-II is more specific to NADH compared to NAD(P)H dehydrogenases from red beet root mitochondria [NDI (*38*) and NDE (*39*)].

Since mammalian hosts lack NDH-II, this enzyme is a promising target for new antiplasmodial agents. However, inhibitors for NDH-II are rare and mostly unspecific (*34*). Fry *et al.* (*11*) examined effects of inhibitors on ATP level in erythrocytic *P. falciparum* and found that 2-heptyl-4-hydroxyquinoline *N*-oxide (HQNO) and 5-hydroxy-2-methyl-1,4-naphthoquinone (plumbagin) showed antimalarial activities with IC_{50} values of 4.0 and 3.5 μM, respectively. In yeast, quinolone analogues HQNO and aurachin C 0-11 were shown to inhibit NDI1 with the IC_{50} values of 8 and 0.2 μM, respectively (*40*). In this study, we examined effects of HQNO and aurachin C 1-10 (*41*) on NADH:Q_1 reductase activity and determined IC_{50} values to be 2.5 and 0.5 μM, respectively (Fig. 5). Our data indicate that the quinolone analogues are potent inhibitors for *Plasmodium* NDH-II. Trifluoroperazine, the uncompetitive inhibitor in terms of Q_2 for *Mycobacterium tuberculosis* NDH-II (IC_{50} = 12 μM) (*42*), reduced the NADH:Q_1 reductase activity to 26% of the control at 100 μM.

DISCUSSION

Properties of Plasmodium Complex II—Parasitic nematodes adapted to hypoxic host environments, have modified respiratory chain, where isoforms of complex II serve as fumarate reductase (*43*, *44*). Kinetic properties of *P. y. yoelii* complex II are similar to those of mammalian enzymes and thus suitable for catalysing the

Table 2. **Effects of quinone-binding site inhibitors on SQR activity of *P. y. yoelii* mitochondria.**

100 μM inhibitor	*P. y. yoelii* mitochondria	Rat liver mitochondria
Control	100%	100%
Atpenin A5	<0.4	<0.05
Carboxin	<0.4	<0.05
Flutoranil	58	22
TTFA	80	12
HQNO	54	94
Plumbagin	52	98
DNP-17	67	99

Control activities (mean ± SD) were 2.66 ± 0.02 (*P. y. yoelii*) and 180 ± 5 (rat liver) mU/mg protein.

forward reaction of TCA cycle (i.e. the oxidation of succinate). It should be noted that *Plasmodium* complex II was more resistant to known quinone-binding site inhibitors for mammalian complex II (Table 2), probably due to the divergence of membrane anchor subunits of *Plasmodium* complex II.

From the whole cell lysate of *P. falciparum*, Suraveratum *et al.* (*28*) purified complex II as the Fp/Ip heterodimer with an apparent molecular weight of 90 kDa and claimed that it has a much lower K_m value (3 μM) for succinate and plumbagin-sensitive SQR activity. However, the concentration (0.2%) of octyl glucoside used for the isolation of *P. falciparum* complex II was not enough for the solubilization of membrane proteins (i.e. critical micell concentration of octyl glucoside is 0.73%). Octyl glucoside likely dissociates the Fp/Ip dimer from the membrane anchor and the aerobic isolation of the Fp/Ip dimer would damage the iron–sulphur clusters in Ip. Thus, SQR activity of such preparations need to be carefully examined.

Plasmodium CybL and CybS are still not annotated in the current database (*6*, *7*), likely due to the divergence from ortholog sequences. However, 2D–PAGE analysis (Fig. 3), SQR activity (Fig. 1, refs. *20*, *25*) and the structure of quinone-binding site in complex II (*30–32*) support the presence of these membrane anchor subunits in *Plasmodium* spp. In membrane anchors of complex II, "$Rx_{16}Sx_2HR$" (helix I) and '$YHx_{10}D$' (helix II) motifs in CybL and '$LHx_{10}DY$' (helix II) motif in CybS are conserved for quinone/haem binding. And only such motifs are conserved in protist membrane anchors (*45*). One candidates for *P. y. yoelii* CybL (accession no. XP_731082, 10,086 Da) and one candidate for CybS (accession no. XP_726783, 10,379 Da) can be identified from 3,310 ORFs shared by *P. falciparum* and *P. y. yoelii* on the basis of the size (<200 amino acid residues), the presence of transmembrane segments (≤3), and the quinone/haem-binding motifs. PyCybL and PyCybS have two transmembrane regions and contain the quinone/haem-binding motifs, '$Rx_{14}Sx_2HY$' and '$YYx_{10}DY$' motifs and '$Yx_{10}G$' motif, respectively. In *S. cerevisiae* strain S288C (Baker's yeast), CybS (accession no. NP_010463) uses the $Yx_{10}DY$ motif, and the His-to-Tyr mutant of the CybL $YHx_{10}D$ motif retained a half of the enzyme activity and haem (*46*). Thus, in *Plasmodium* CybL and CybS, Tyr could also substitute the role of the conserved His residue in membrane anchor subunits. Although it has to be tested by protein chemically in future studies, our data support that the subunit structure of *Plasmodium* complex II is similar to that of mammalian complex II.

Properties of Plasmodium NDH-II—Previously, Krungkrai *et al.* (*47*) isolated mitochondrial complex I from *P. falciparum* and *P. berghei* as a 130-kDa complex containing 38- and 33-kDa subunits. They claimed that NADH:ubiquinone-8 reductase activity was sensitive to rotenone (IC_{50} = 12 μM) and plumbagin (IC_{50} = 6 μM). However, NDH-I is not encoded by the *Plasmodium* genomes (*6*, *7*) and concentrations of *n*-octyl glucoside used for the solubilization and purification were below its critical micelle concentration (CMC) where *n*-octyl glucoside cannot serve as a detergent. Alternative NADH dehydrogenase NDH-II is a rotenone-insensitive single-subunit enzyme (*15*, *34*) and the apparent molecular weights and subunit structure of *P. falciparum* (acc. no. XP_001352022 and MW 61,670) and *P. y. yoelii* (acc. no. XP_731423, MW 66,156) NDH-II are totally different from those reported by Krungkrai *et al.* (*47*). The IC_{50} value of mouse liver mitochondria for rotenone (8.4 μM; Table 3 in ref. 47) was three orders of magnitude higher than the IC_{50} reported for mammalian enzymes (*26*). Recently, Biagini *et al.* (*15*) used the whole cell lysate of *P. falciparum* and claimed that PfNDH-II was inhibited by diphenylene iodonium chloride (DPI, IC_{50} of 15–25 μM) and diphenyl iodonium chloride (IDP, IC_{50} = 66 μM). As pointed out by Vaidya *et al.* (*48*), the IC_{50} for the enzyme was 100- and 10-fold higher than those for the growth inhibition and other NADH oxidases in the lysate may contribute to the activity. Very recently, it was reported that purified recombinant PfNDH-II was not inhibited by known NDH-I inhibitors and flavoenzyme inhibitors (DPI and IDP) (Dong, C., Patel, V., Clardy, J., and Wirth, D., personal communication). Thus, previous studies on *Plasmodium* NDH-II need to be reexamined. Our data indicate that *Plasmodium* NDH-II is a member of internal NDH-II (Ndi), which reoxidizes NADH in the mitochondrial matrix. Recently, Saleh *et al.* (*49*) demonstrated the antiplasmodial activity (IC_{50} = 14 nM) of 1-hydroxy-2-dodecyl-4(1*H*)quinolone (HDQ), which has been identified as the potent inhibitor for *Y. lipolytica* NDE (IC_{50} = 0.2 μM) (*50*), demonstrating that *Plasmodium* NDH-II is a promising target for new drugs.

Oxidative Phosphorylation in Plasmodium Mitochondria—For a long time, it has been assumed that *Plasmodium* mitochondria cannot carry out oxidative phosphorylation (*4*, *5*) because of a lack of membrane anchor subunits of ATP synthase (*9*, *11*). Oxidative phosphorylation, succinate respiration (*8*, *17*), and effects of respiratory complex inhibitors on the generation of membrane potential (*16*) in rodent malaria mitochondria support the notion that *Plasmodium* mitochondria are fully capable of oxidative phosphorylation. Careful analysis of current genome databases (*6*, *7*) with partial subunits sequences of *Crithidia fasciculata* (*51*) and *Leishmania tarentolae* (*52*) could identify ten subunits of *P. falciparum* F_oF_1-ATP synthase, including membrane anchor subunits *a* (XP_001347344) and *b* (XP_001348969) (Mogi, T. and Kita, K., unpublished

results), which are found to be highly divergent from eukaryotic and bacterial counterparts. Thus, all canonical subunits of complex II and ATP synthase are present in *Plasmodium* spp., and malaria parasites can yield energy *via* oxidative phosphorylation. The *in vivo* expression profiles of parasites derived from infected patients showed the up-regulation of these enzymes under conditions similar to starvation in yeast (*18*).

CONCLUSION

We isolated active mitochondria from rodent malaria *P. y. yoelii* from infected mouse erythrocytes and characterized complex II and NDH-II. *Plasmodium* complex II is the four-subunit enzyme but its quinone-reduction site in the membrane anchor subunits seems structurally different from that of mammalian enzyme. *Plasmodium* NDH-II showed enzymatic properties similar to those of NDI and quinolones were found to be potent inhibitors. Alternative respiratory enzymes, which are absent in mammalian mitochondria, are as promising targets for new antibiotics (*53*, *54*). We hope that our findings will help understanding of energy metabolism in malaria parasites and the development of new antimalarial drugs.

FUNDING

This study was supported in part by a grant-in-aid for scientific research (20570124 to T.M.), scientific research on Priority Areas (18073004 to K.K.) and Creative Scientific Research (18GS0314 to K.K.) from the Japanese Ministry of Education, Science, Culture, Sports, and Technology. We thank Dr H. Ohtsuki (Ehime University) for *P. y. yoelii* strain 17XL, Dr. D. Wirth (Harvard School of Public Health) for the use of unpublished results prior to publication, and Ministry of Health, Labour and Welfare for financial supports.

CONFLICT OF INTEREST

None declared.

REFERENCES

1. World Health Organization (2007) Malaria Elimination. A field manual for low and moderate endemic countries. World Health Organization, Geneva, Switzerland
2. Hyde, J.E. (2005) Drug-resistant malaria. *Trends Parasitol.* **21**, 494–498
3. Sherman, I.W. (1998) Carbohydrate metabolism of asexual stages. in *Malaria, Parasite Biology, Pathogenesis and Protection* (Sherman, I.W., ed.), pp. 135–143, ASM Press, Washington, DC
4. Vaidya, A.B. (1998) Mitochondrial physiology as a target for atovaquone and other antimalarials. in *Malaria, Parasite Biology, Pathogenesis and Protection* (Sherman, I.W., ed.), pp. 355–368, ASM Press, Washington, DC
5. Van Dooren, G.G., Stimmler, L.M., and McFadden, G.I. (2006) Metabolic maps and functions of the *Plasmodium* mitochondrion. *FEMS Microbiol. Rev.* **30**, 596–630
6. Gardner, M.J., Hall, N., Fung, E., White, O., Berriman, M., Hyman, R.W., Carlton, J.M., Pain, A., Nelson, K.E., Bowman, S., Paulsen, I.T., James, K., Eisen, J.A., Rutherford, K., Salzberg, S.L., Craig, A., Kyes, S., Chan, M.S., Nene, V., Shallom, S.J., Suh, B., Peterson, J., Angiuoli, S., Pertea, M., Allen, J., Selengut, J., Haft, D., Mather, M.W., Vaidya, A.B., Martin, D.M., Fairlamb, A.H., Fraunholz, M.J., Roos, D.S., Ralph, S.A., McFadden, G.I., Cummings, L.M., Subramanian, G.M., Mungall, C., Venter, J.C., Carucci, D.J., Hoffman, S.L., Newbold, C., Davis, R.W., Fraser, C.M., and Barrell, B. (2002) Genome sequence of the human malaria parasite *Plasmodium falciparum*. *Nature* **419**, 498–511
7. Carlton, J.M., Angiuoli, S.V., Suh, B.B., Kooij, T.W., Pertea, M., Silva, J.C., Ermolaeva, M.D., Allen, J.E., Selengut, J.D., Koo, H.L., Peterson, J.D., Pop, M., Kosack, D.S., Shumway, M.F., Bidwell, S.L., Shallom, S.J., van Aken, S.E., Riedmuller, S.B., Feldblyum, T.V., Cho, J.K., Quackenbush, J., Sedegah, M., Shoaibi, A., Cummings, L.M., Florensk, L., Yatesk, J.R., Raine, J. D., Sinden, R.E., Harris, M.A., Cunningham, D.A., Preiser, P.R., Bergman, L.W., Vaidya, A.B., van Lin, L.H., Janse, C.J., Waters, A.P., Smith, H.O., White, O.R., Salzberg, S.L., Venter, J.C., Fraser, C.M., Hoffman, S.L., Gardner, M.J., and Carucci, D.J. (2002) Genome sequence and comparative analysis of the model rodent malaria parasite *Plasmodium yoelii yoelii*. *Nature* **419**, 512–519
8. Uyemura, S.A., Luo, S., Vieira, M., Moreno, S.N., and Docampo, R. (2004) Oxidative phosphorylation and rotenone-insensitive malate- and NADHquinone oxidoreductases in *Plasmodium yoelii yoelii* mitochondria *in situ*. *J. Biol. Chem.* **279**, 385–393
9. Matsushita, K., Ohnishi, T., and Kaback, H.R. (1987) NADH-ubiquinone oxidoreductases of the *Escherichia coli* aerobic respiratory chain. *Biochemistry* **26**, 7732–7737
10. Takeo, S., Kokaze, A., Ng, C.S., Mizuchi, D., Watanabe, J.I., Tanabe, K., Kojima, S., and Kita, K. (2000) Succinate dehydrogenase in *Plasmodium falciparum* mitochondria: molecular characterization of the *SDHA* and *SDHB* genes for the catalytic subunits, the flavoprotein (Fp) and iron–sulfur (Ip) subunits. *Mol. Biochem. Parasitol.* **107**, 191–205
11. Fry, M., Webb, E., and Pudney, M. (1990) Effect of mitochondrial inhibitors on adenosinetriphosphate levels in *Plasmodium falciparum*. *Comp. Biochem. Physiol. B* **96**, 775–782
12. Vaidya, A.B. and Mather, M.W.A. (2005) Post-genomic view of the mitochondrion in malaria parasites. *Curr. Top. Microbiol. Immunol.* **295**, 233–250
13. Painter, H.J., Morrisey, J.M., Mather, M.W., and Vaidya, A.B. (2007) Specific role of mitochondrial electron transport in blood-stage *Plasmodium falciparum*. *Nature* **446**, 88–91
14. Fry, M. and Pudney, M. (1992) Site of action of the antimalarial hydroxynaphthoquinone, 2-[trans-4-(4′-chlorophenyl)cyclohexyl]-3-hydroxy-1,4-naphthoquinone (566C80). *Biochem. Pharmacol.* **43**, 1545–1453
15. Biagini, G.A., Viriyavejakul, P., O'Neill, P.M., Bray, P.G., and Ward, S.A. (2006) Functional characterization and target validation of alternative Complex I of *Plasmodium falciparum* mitochondria. *Antimicrob. Agents Chemother.* **50**, 1841–1851
16. Srivastava, I.K., Rottenberg, H., and Vaidya, A.B. (1997) Atovaquone, a broad spectrum antiparasitic drug, collapses mitochondrial membrane potential in malarial parasite. *J. Biol. Chem.* **272**, 3961–3966
17. Uyemura, S.A., Luo, S., Moreno, S.N.J., and Docampo, R. (2000) Oxidative phosphorylation, Ca^{2+} transport, and fatty acid-induced uncoupling in malaria parasites mitochondria. *J. Biol. Chem.* **275**, 9709–9715
18. Daily, J.P., Scanfeld, D., Pochet, N., Roch, K.L., Plouffe, D., Kamel, M., Sarr, O., Mboup, S., Ndir, O., Wypij, D., Lavasseur, K., Thomas, E., Tamayo, P., Dong, C., Zhou, Y., Lander, E.S., Ndiaye, D., Wirth, D., Winzeler, E.A., Mesirov, J.P., and Regev, A. (2007)

Distinct physiological states of *Plasmodium falciparum* in malaria-infected patients. *Nature* **450**, 1091–1095
19. Homewood, C.A. and Neame, K.D. (1976) Comparison of methods used for removal of white cells from malaria-infected blood. *Ann. Trop. Med. Parasitol.* **70**, 249–251
20. Takashima, E., Takamiya, S., Takeo, S., Mi-ichi, F., Amino, H., and Kita, K. (2001) Isolation of mitochondria from *Plasmodium falciparum* showing dihydroorotate dependent respiration. *Parasitol. Int.* **50**, 273–278
21. Johnson, D. and Lardy, H. (1967) Isolation of liver or kidney mitochondria in *Methods Enzymol.* Vol. 10, (Estabrook, R.W. and Pullman, M.E., eds.), pp. 94–96, Academic Press, New York
22. Mogi, T., Ui, H., Shiomi, K., Ōmura, S., and Kita, K. (2008) Gramicidin S identified as a potent inhibitor for cytochrome *bd*-type quinol oxidase. *FEBS Lett.* **582**, 2299–2302
23. Wittig, I., Karas, M., and Schagger, H. (2007) High resolution clear native electrophoresis for in-gel functional assays and fluorescence studies of membrane protein complexes. *Mol. Cell Proteomics* **6**, 1215–1122
24. Kobayashi, T., Sato, S., Takamiya, S., Komaki-Yasuda, K., Yano, K., Hirata, A., Onitsuka, A., Hata, M., Mi-ichi, F., Tanaka, T., Hase, T., Miyajima, A., Kawazu, S., Watanabe, Y., and Kita, K. (2007) Mitochondria and apicoplast of *Plasmodium falciparum*: behaviour on subcellular fractionation and the implication. *Mitochondrion* **7**, 125–132
25. Mi-Ichi, F., Miyadera, H., Kobayashi, T., Takamiya, S., Waki, S., Iwata, S., Shibata, S., and Kita, K. (2005) Parasite mitochondria as a target of chemotherapy: inhibitory effect of licochalcone A on the *Plasmodium falciparum* respiratory chain. *Ann. NY Acad. Sci.* **1056**, 46–54
26. Ueno, H., Miyoshi, H., Ebisui, K., and Iwamura, H. (1994) Comparison of the inhibitory action of natural rotenone and its stereoisomers with various NADH-ubiquinone reductases. *Eur. J. Biochem.* **225**, 411–417
27. Tushurashvili, P.R., Gavrikova, E.V., Ledenev, A.N., and Vinogradov, A.D. (1985) Studies on the succinate dehydrogenating system. Isolation and properties of the mitochondrial succinate-ubiquinone reductase. *Biochim. Biophys. Acta* **809**, 145–159
28. Miyadera, H., Shiomi, K., Ui, H., Yamaguchi, Y., Masuma, R., Tomoda, H., Miyoshi, H., Osanai, A., Kita, K., and Omura, S. (2003) Atpenins, potent and specific inhibitors of mitochondrial complex II (succinate-ubiquinone oxidoreductase). *Proc. Natl Acad. Sci. USA* **100**, 473–477
29. Suraveratum, N., Krungkrai, S.R., Leangaramgul, P., Prapunwattana, P., and Krungkrai, J. (2000) Purification and characterization of *Plasmodium falciparum* succinate dehydrogenase. *Mol. Biochem. Parasitol.* **105**, 215–222
30. Yankovskaya, V., Horsefield, R., Tornroth, S., Luna-Chavez, C., Miyoshi, H., Leger, C., Byrne, B., Cecchini, G., and Iwata, S. (2003) Architecture of succinate dehydrogenase and reactive oxygen species generation. *Science* **299**, 700–704
31. Sun, F., Huo, X., Zhai, Y., Wang, A., Xu, J., Su, D., Bartlam, M., and Rao, Z. (2005) Crystal structure of mitochondrial respiratory membrane protein complex II. *Cell* **121**, 1043–1057
32. Huang, L.S., Sun, G., Cobessi, D., Wang, A.C., Shen, J.T., Tung, E.Y., Anderson, V.E., and Berry, E.A. (2006) 3-Nitropropionic acid is a suicide inhibitor of mitochondrial respiration that, upon oxidation by Complex II, forms a covalent adduct with a catalytic base arginine in the active site of the enzyme. *J. Biol. Chem.* **281**, 5965–5972
33. Schägger, H. and Pfeiffer, K. (2000) Supercomplexes in the respiratory chains of yeast and mammalian mitochondria. *EMBO J.* **19**, 1777–1783
34. Kerscher, S.J. (2000) Diversity and origin of alternative NADH:ubiquinone oxidoreductase. *Biochim. Biophys. Acta* **1459**, 274–283
35. De Vries, S. and Grivell, L.A. (1988) Purification and characterization of a rotenone-insensitive NADH:Q_6 oxidoreductase from mitochondria of *Saccharomyces cerevisiae*. *Eur. J. Biochem.* **176**, 377–341
36. Björklöf, K., Zickermann, V., and Finel, M. (2000) Purification of the 45 kDa, membrane bound NADH dehydrogenase of *Escherichia coli* (NDH-2) and analysis of its interaction with ubiquinone analogs. *FEBS Lett.* **467**, 105–110
37. Kerscher, S.J., Okun, J.G., and Brandt, U. (1999) A single external enzyme confers alternative NADH:ubiquinone oxidoreductase activity in *Yarrowia lipolytica*. *J. Cell Sci.* **112**, 2347–2354
38. Rasmusson, A.G., Fredlund, K.M., and Møller, I.M. (1993) Purification of a rotenone-insensitive NAD(P)H dehydrogenase from the inner surface of red beetroot mitochondria. *Biochim. Biophys. Acta* **1141**, 107–110
39. Luethy, M.H., Thelen, J.J., Knudten, A.F., and Elthon, T.E. (1995) Purification, characterization, and submitochondrial localization of a 58-kilodalton NAD(P)H dehydrogenase. *Plant Physiol.* **107**, 443–450
40. Yamashita, T., Nakamaru-Ogiso, E., Miyoshi, H., Matsuo-Yagi, A., and Yagi, T. (2007) Roles of bound quinone in the single subunit NADH-quinone oxidoreductase (Ndi1) from *Saccharomyces cerevisiae*. *J. Biol. Chem.* **282**, 6012–6020
41. Miyoshi, H., Takegami, K., Sakamoto, K., Mogi, T., and Iwamura, H. (1999) Characterization of the ubiquinol oxidation sites in cytochromes *bo* and *bd* from *Escherichia coli* using aurachin C analogues. *J. Biochem.* **125**, 138–142
42. Yano, T., Li, L.-S., Weinstein, E., The, J.-S., and Rubin, H. (2006) Steady-state kinetics and inhibitory action of antitubercular phenothiazines on *Mycobacterium tuberculosis* type-II NADH-menaquinone oxidoreductase (NDH-2). *J. Biol. Chem.* **281**, 11456–11463
43. Roos, M.H. and Tielens, A.G.M. (1994) Differential expression of two succinate dehydrogenase subunit-B genes and a transition in energy metabolism during the development of the parasitic nematode *Haemonchus contortus*. *Mol. Biochem. Parasitol.* **66**, 273–281
44. Saruta, F., Kuramochi, T., Nakamura, K., Takamiya, S., Yu, Y., Aoki, T., Sekimizu, K., Kojima, S., and Kita, K. (1995) Stage-specific isoforms of complex II (succinate-ubiquinone oxidoreductase) in mitochondria from the parasitic nematode, *Ascaris suum*. *J. Biol. Chem.* **270**, 928–932
45. Morales, J., Mogi, T., and Kita, K. (2008) Divergence in structure of mitochondrial respiratory Complex II (succinate-ubiquinone reductase) revealed by protozoan enzymes. *Biochim. Biophys. Acta* **1777**, S94–S95
46. Oyedotun, K.S. and Lemire, B.D. (1999) The *Saccharomyces cerevisiae* succinate-ubiquinone oxidoreductase. Identification of Sdh3p amino acid residues involved in ubiquinone binding. *J. Biol. Chem.* **274**, 23956–23962
47. Krungkrai, J., Kanchanarithisak, R., Krungkrai, S.R., and Sunant Rochanakij, S. (2002) Mitochondrial NADH dehydrogenase from *Plasmodium falciparum* and *Plasmodium berghei*. *Exp. Parasitol.* **100**, 54–61
48. Vaidya, A.B., Painter, H.J., Morrisey, J.M., and Mather, M.W. (2008) The validity of mitochondrial dehydrogenases as antimalarial drug targets. *Trends Parasitol.* **24**, 8–9
49. Saleh, A., Friesen, J., Baumeister, S., Gross, G., and Bohne, W. (2007) Growth inhibition of *Toxoplasma gondii* and *Plasmodium falciparum* by nanomolar concentrations of 1-hydroxy-2-dodecyl-4(1*H*)quinolone, a high-affinity inhibitor of alternative (type II) NADH dehydrogenases. *Antimicrob. Agents Chemother.* **51**, 1217–1222
50. Eschemann, A., Galkin, A., Oettmeier, W., Brandt, U., and Kerscher, S. (2005) HDQ (1-hydroxy-2-dodecyl-4(1*H*)quinolone), a high affinity inhibitor for mitochondrial

alternative NADH dehydrogenase: evidence for a ping-pong mechanism. *J. Biol. Chem.* **280**, 3138–3142

51. Speijer, D., Breek, C.K., Muijsers, A.O., Hartog, A.F., Berden, J.A., Albracht, S.P., Samyn, B., van Beeumen, J., and Benne, R. (1997) Characterization of the respiratory chain from cultured *Crithidia fasciculate*. *Mol. Biochem. Parasitol.* **85**, 171–186
52. Nelson, R.E., Aphasizheva, I., Falick, A.M., Nebohacova, M., and Simpson, L. (2004) The I-complex in *Leishmania tarentolae* is an uniquely-structured F_1-ATPase. *Mol. Biochem. Parasitol.* **135**, 221–224
53. Minagawa, N., Yabu, Y., Kita, K., Nagai, K., Ohta, N., Meguro, K., Sakajo, S., and Yoshimoto, A. (1997) An antibiotic, ascofuranone, specifically inhibits respiration and in vitro growth of long slender bloodstream forms of *Trypanosoma brucei brucei*. *Mol. Biochem. Parasitol* **84**, 271–280
54. Saimoto, H., Shigemasa, Y., Kita, K., Yabu, Y., Hosokawa, T., and Yamamoto, M. (2007) Novel phenol derivatives and antitrypanosoma preventive/therapeutic agent comprising the same as active ingredient. U.S. Patent 20070208078

Biochimica et Biophysica Acta 1787 (2009) 129–133

Contents lists available at ScienceDirect

Biochimica et Biophysica Acta

journal homepage: www.elsevier.com/locate/bbabio

Antibiotics LL-Z1272 identified as novel inhibitors discriminating bacterial and mitochondrial quinol oxidases

Tatsushi Mogi [a,*], Hideaki Ui [b], Kazuro Shiomi [b], Satoshi Ōmura [b], Hideto Miyoshi [c], Kiyoshi Kita [a]

[a] Department of Biomedical Chemistry, Graduate School of Medicine, The University of Tokyo, Hongo, Bunkyo-ku, Tokyo 113-0033, Japan
[b] Kitasato Institute for Life Sciences and Graduate School of Infection Control Sciences, Kitasato University, Shirokane, Minato-ku, Tokyo 108-8641, Japan
[c] Division of Applied Life Sciences, Graduate School of Agriculture, Kyoto University, Sakyo-ku, Kyoto 606-8502, Japan

ARTICLE INFO

Article history:
Received 9 October 2008
Received in revised form 21 November 2008
Accepted 26 November 2008
Available online 10 December 2008

Keywords:
Quinol oxidase
Inhibitor
Natural antibiotic
Escherichia coli
Trypanosoma brucei
Alternative oxidase

ABSTRACT

To counter antibiotic-resistant bacteria, we screened the Kitasato Institute for Life Sciences Chemical Library with bacterial quinol oxidase, which does not exist in the mitochondrial respiratory chain. We identified five prenylphenols, LL-Z1272β, γ, δ, ε and ζ, as new inhibitors for the *Escherichia coli* cytochrome *bd*. We found that these compounds also inhibited the *E. coli bo*-type ubiquinol oxidase and trypanosome alternative oxidase, although these three oxidases are structurally unrelated. LL-Z1272β and ε (dechlorinated derivatives) were more active against cytochrome *bd* while LL-Z1272γ, δ, and ζ (chlorinated derivatives) were potent inhibitors of cytochrome *bo* and trypanosome alternative oxidase. Thus prenylphenols are useful for the selective inhibition of quinol oxidases and for understanding the molecular mechanisms of respiratory quinol oxidases as a probe for the quinol oxidation site. Since quinol oxidases are absent from mammalian mitochondria, LL-Z1272β and δ, which are less toxic to human cells, could be used as lead compounds for development of novel chemotherapeutic agents against pathogenic bacteria and African trypanosomiasis.

1. Introduction

The emergence of antibiotic-resistant strains of major pathogenic bacteria such as *Staphylococcus aureus* is an increasingly serious public health concern [1]. To evade bacterial drug-resistance mechanisms, new effective chemotherapeutic agents, which have novel mechanisms of action as well as different cellular targets compared with conventional antibiotics, need to be developed [2].

Cytochromes *bo* (CyoABCD) and *bd* (CydAB) are two terminal quinol oxidases of the aerobic respiratory chain in *Escherichia coli* and many other bacteria [3,4 for reviews]. Although they are structurally unrelated, both generate proton-motive force through the oxidation of quinols coupled to dioxygen reduction. Cytochrome *bo* is a proton-pumping heme–copper terminal oxidases and is predominantly expressed under highly aerated growth conditions. In contrast, cytochrome *bd* is a predominant terminal oxidase under microaerophilic growth conditions and performs a variety of physiological functions such as microaerophilic respiration and protection against oxygen stress. Further, cytochrome *bd* and its variant cyanide-insensitive oxidase (CioAB) play a key role in survival and adaptation of pathogenic bacteria that encounter host environments where dioxygen is progressively limited [5–9].

In long slender bloodstream forms of the parasitic protist *Trypanosoma brucei*, which causes sleeping sickness in human and nagana in livestock, mitochondrial respiratory Complexes III and IV are down-regulated and alternative quinol oxidase (AOX) serves as a terminal oxidase [10,11]. AOX is a di-iron family protein bound to the matrix side of the inner membrane and cannot generate the proton-motive force. All three quinol oxidases have no counterparts in mammalian mitochondria, thus they are potential targets for novel antimicrobial chemotherapeutics. In fact, we previously identified ascofuranone (AF), a prenylphenol isolated from a phytopathogenic fungus *Ascochyta viciae* [12], as a potent inhibitor for the growth of *T. brucei* and trypanosome AOX (noncompetitive inhibition with IC_{50} of 2 nM) [13,14].

By screening of hundreds of natural antibiotics in the Kitasato Institute for Life Sciences Chemical Library [15] with the *E. coli* cytochrome *bd*, we found that LL-Z1272γ has potent inhibititory activity. We extended our screening to related compounds and found that antibiotics LL-Z1272β, γ, δ, ε and ζ (Fig. 1), prenylphenols isolated from the fungus *Verticillum* sp. FO-2787 [16], are a unique set of natural compounds that can discriminate and inhibit alternative respiratory quinol oxidases. Thus, antibiotics LL-Z1272 are useful probes for understanding of molecular mechanisms of quinol oxidases and we hope that our findings contribute to the development of new antibiotics.

2. Materials and methods

2.1. Isolation or source of antibiotics and inhibitors

LL-Z1272β, γ, δ, ε and ζ were isolated from the cultured mycelium *Verticillum* sp. FO-2787 [16]. Antibiotics LL-Z1272α, β, γ,

* Corresponding author. Tel.: +81 3 5841 8202; fax: +81 3 5841 3444.
E-mail address: tmogi@m.u-tokyo.ac.jp (T. Mogi).

0005-2728/$ – see front matter © 2008 Elsevier B.V. All rights reserved.
doi:10.1016/j.bbabio.2008.11.016

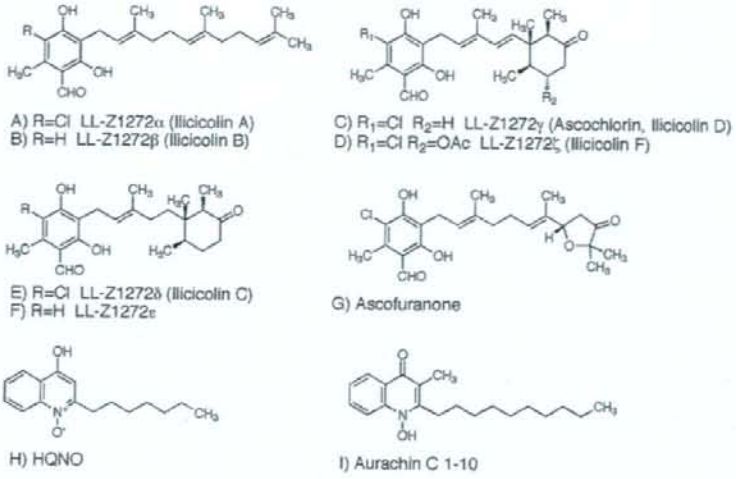

Fig. 1. Structures of antibiotics LL-Z1272 and related natural compounds.

δ, ε and ζ have been originally isolated from an imperfect fungus *Fusarium* sp. as inhibitors for the growth of the protist *Tetrahymena pyriformis* [17]. Ilicicolin A, B, D, C, and F isolated from the fungus *Cylindrocladium ilicicola* [18] are also identical to LL-Z1272α, β, γ, δ, and ζ, respectively [19]. AF and piericidin A were kind gifts from Drs. Masaichi Yamamoto (aRigen Pharmaceuticals. Inc.) and Shigeo Yoshida (Institute of Physical and Chemical Research), respectively. Synthesis of aurachin C 1-10 was described previously [20]. Antimycin A_1 and 2-heptyl-4-hydroxyquinoline *N*-oxide (HQNO) were purchased from Sigma.

2.2. Preparation of cytoplasmic membrane vesicles and purification of cytochrome bo

Cytochrome *bd*-overproduced membranes were isolated from *E. coli* ST4683/pNG2 (Δ*cyo* Δ*cyd*/*cyd*$^+$ Tet^R), which can overproduce *bd*-type quinol oxidase as the sole terminal oxidase [21]. Heme *d* content was 2.1±0.1 nmol/mg protein (*i.e.* approximately 20% of membrane proteins). Cytochrome *bo*-type quinol oxidase was purified from cytoplasmic membranes of *E. coli* GO103/pHN3795-1 (*cyo*$^+$ Δ*cyd*/*cyo*$^+$ Amp^R), as described previously [22]. Trypanosome AOX-overproduced membranes were isolated from *E. coli* FN102 (BL21 (DE3) Δ*hemA*)/pTvAOX, which can express *Trypanosoma vivax* AOX as the sole functional quinol oxidase [23]. The expression level of AOX was estimated to be ~5% of membrane proteins by SDS-polyacrylamide gel electrophoresis.

2.3. Quinol oxidase assay

The activity of the *E. coli* quinol oxidases was determined at 25 °C with a V-660 double monochromatic spectrophotometer (JASCO, Tokyo, Japan) with data acquisition at 0.05 s. The reaction mixture (1 ml) contained 50 mM potassium phosphate (pH 6.5), and 0.02% Tween 20 (protein grade, Calbiochem) [24]. Enzyme concentrations were 2.4 nM for cytochrome *bd* and 2 nM for cytochrome *bo*. Reactions were started by addition of ubiquinol-1 (Q_1H_2) at a final concentration of 100 μM, and the activity was calculated by using a molar extinction coefficient of 12,300 at 278 nm. The activity of *T. vivax* AOX was measured in 50 mM Tris–HCl (pH 7.4)–0.1% sucrose monolaurate (Mitsubishi-Kagaku Foods Co., Tokyo, Japan). Enzyme kinetics were analyzed based on the modified *ping-pong bi-bi* mechanism for cytochrome *bd* [21] or the Michaelis–Menten mechanism for cytochrome *bo* and *T. vivax* AOX, by using KaleidaGraph ver. 4.0 (Synergy Software, Reading, PA).

2.4. Dose–response analysis

Duplicate assays were performed at each concentration with two independent preparations of membranes. Dose-response data were analyzed by the nonlinear regression curve-fitting with KaleidaGraph ver. 4.0 as described previously [24]. IC_{50} values in the presence of 100 μM Q_1H_2 were estimated by using the equation for the relative residual activity; $v = 1/(1+([\text{Inhibitor}]/IC_{50})^n)$ where n is the Hill coefficient [24].

3. Results

3.1. Analysis of inhibition of cytochrome bd by antibiotics LL-Z1272

In the course of our screening for inhibitors against the *E. coli* cytochrome *bd*, we identified LL-Z1272γ as an antibiotic that suppressed the Q_1H_2 oxidation by the cytochrome *bd*-overproduced membranes (84% inhibition at 5 μg/ml) greater than antimycin A (50%), a non-competitive inhibitor of cytochrome *bd* [25]. We extended our screening with antibiotics LL-Z1272β, γ, δ, ε and ζ, prenylphenols isolated from *Verticillum* sp. FO-2787 [16], and found that LL-Z1272β and ε were more potent inhibitors for cytochrome *bd*. These compounds do not have a chlorine atom at position 5 of the phenol ring (Fig. 1), and the cyclohexanone ring of LL-Z1272ε slightly increased the binding affinity to cytochrome *bd* (Table 1). The 50% inhibitory concentrations (IC_{50}) for LL-Z1272β and ε (dechlorinated derivatives) were determined to be 2.1 and 1.1 μM (average values of two independent preparations), respectively, and are one-order of magnitude smaller than those of LL-Z1272γ, δ and ζ (chlorinated derivatives) (Table 1). The IC_{50} values for known inhibitors for cytochrome *bd* [20,25–27] are 10 μM for piericidin A, 5 μM for antimycin A, 1 μM for HQNO, and 8.3 nM for aurachin C 1–10.

Table 1
Summary on IC_{50} values of quinol oxidase inhibitors for the *E. coli* cytochrome *bd* and *bo* and *T. vivax* AOX

Compounds	Cytochrome bd[a]	Cytochrome bo[b]	trypanosome AOX[c]
LL-Z1272β	2.1±0.1[d]	1.2±0.1	0.18±0.02
LL-Z1272γ	81±17	0.082±0.016	0.015±0.001
LL-Z1272δ	32±4	0.28±0.02	0.046±0.004
LL-Z1272ε	1.1±0.1	7.2±0.7	0.65±0.09
LL-Z1272ζ	85±7	0.37±0.02	0.43±0.02
Ascofuranone	47±10	0.062±0.003	0.0049±0.0002
Aurachin C 1–10	0.0083±0.0003	0.0023±0.0001	28±2

[a] The *E. coli* cytochrome *bd*-overproduced membranes.
[b] The purified *E. coli* cytochrome *bo*.
[c] The *T. vivax* AOX-overproduced membranes.
[d] μM.

3.2. Kinetic analysis of inhibition of cytochrome bd by LL-Z1272β and ε

Effects of LL-Z1272β and ε on the Q_1H_2 oxidation by cytochrome *bd* were further analyzed kinetically. Control data were analyzed based on the modified *ping-pong bi-bi* mechanism by assuming the stabilization of dioxygen reduction intermediates [28] and apparent K_m and V_{max} values for the control were determined to 50 μM and 2364 Q_1H_2/enzyme/s, respectively, in 50 mM potassium phosphate (pH 6.5)–0.02% Tween 20 [24] (Fig. 2). In the presence of inhibitors, reactions followed the Michaelis–Menten kinetics (Fig. 2). LL-Z1272β acts as a noncompetitive inhibitor with K_i=7.6±2.5 μM while LL-Z1272ε serves as a competitive inhibitor with K_i=1.00±0.03 μM (Fig. 2).

3.3. Dose–response analysis of inhibition of cytochrome bo by antibiotics LL-Z1272

In contrast to *bd*-type oxidase, the Q_1H_2 oxidase activity of the *E. coli* cytochrome *bo* was more sensitive to chlorinated derivatives, LL-Z1272γ, ε and ζ. IC_{50} values for LL-Z1272β, γ, δ, ε and ζ (averages from two preparations) were determined to be 1.2, 0.082, 0.28, 7.2 and 0.37 μM, respectively (Table 1). The IC_{50} values for known inhibitors for cytochrome *bo* [20,27,29–31] are 0.3 μM for HQNO, 0.14 μM for piericidin A, and 2.3 nM for aurachin C 1–10, showing that cytochrome *bo* is more sensitive to these quinone analogs than cytochrome *bd*. It should be noted that LL-Z1272γ is a very potent inhibitor of cytochrome *bo*.

3.4. Kinetic analysis of inhibition of cytochrome bo by antibiotics LL-Z1272

Effects of LL-Z1272β, γ, δ, and ζ on the Q_1H_2 oxidation by cytochrome *bo* were further analyzed kinetically at different concentrations of inhibitors. Enzyme kinetics were analyzed based on the Michaelis–Menten mechanism [29,31], and we found that the inhibition mechanism was all mixed-type (Fig. 3). It should be noted that due to changes in assay conditions apparent K_m and V_{max} values were shifted to 23 μM and 1035 Q_1H_2/enzyme/s, respectively (Fig. 3), from 50 μM and 515 Q_1H_2/enzyme/s, respectively, in 50 mM Tris–HCl (pH 7.4)–0.1% sucrose monolaurate in our previous study [32].

3.5. Dose–response analysis of inhibition of trypanosome AOX by antibiotics LL-Z1272

Because of the structural similarity of antibiotics LL-Z1272 with trypanocidal AF (Fig. 1), we examined the effects of antibiotics LL-Z1272 on Q_1H_2 oxidase activity of *T. vivax* AOX. From dose–response analysis with the AOX-overproduced *E. coli* membranes, we determined IC_{50} values for LL-Z1272β, γ, δ, ε, ζ, AF and aurachin C1–10 to be 180, 15, 46, 650, 430, 4.9 nM and 28 μM, respectively (Table 1). Our data indicate that 1) the furanone ring of AF is not essential for binding to trypanosome AOX, 2) the 5-chloride group on the phenol ring increases the binding affinity, and 3) aurachin C, the most potent inhibitor for bacterial quinol oxidases (IC_{50}=8.3 and 2.3 nM for the *E. coli* cytochrome *bd* and *bo*, respectively (Table 1)) [20,27], is 2 to 4 order of magnitude less active than the prenylphenols.

3.6. Kinetic analysis of inhibition of trypanosome AOX by antibiotics LL-Z1272

Effects of LL-Z1272β, γ, δ, ε and ζ and AF on enzyme kinetics by *T. vivax* AOX were examined in the presence of detergents. Q_1H_2 oxidation by *T. vivax* AOX followed the Michaelis–Menten kinetics

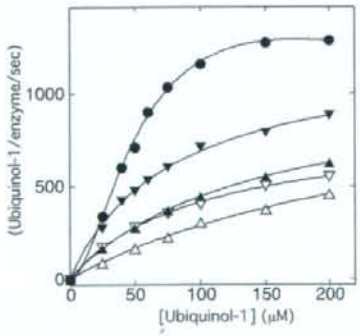

Fig. 2. Effects of antibiotics LL-Z1272 on kinetic parameters for Q_1H_2 oxidation by the *E. coli* cytochrome *bd*. Kinetic analysis was carried out in the absence of inhibitors (●) and the presence of 2 (▼) or 5 (▽) μM LL-Z1272β or 2 (▲) or 5 (△) μM LL-Z1272ε. Control data was analyzed by using the equation $v = SV_{max}/(SS(1+S/K_s)+SK_m+K_mK_m)$ where K_s indicates the constant for substrate inhibition. Data obtained in the presence of inhibitors were analyzed based on the Michaelis–Menten kinetics. The apparent K_m (μM) and V_{max} (Q_1H_2/enzyme) values obtained were 50±4 and 2364±194, respectively, for the control (K_s=381 μM), 79±5 and 1232±33, respectively, for 2 μM LL-Z1272β, 100±5 and 826±21, respectively, for 5 μM LL-Z1272β, 140±3 and 1065±12, respectively, for 2 μM LL-Z1272ε, 287±41 and 1113±107 Q_1H_2/enzyme/s, respectively, for 5 μM LL-Z1272ε, respectively.

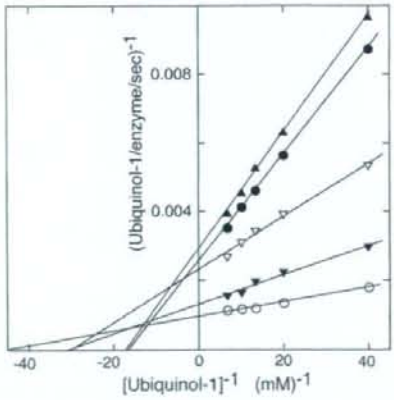

Fig. 3. Effects of antibiotics LL-Z1272 on kinetic parameters for Q_1H_2 oxidation by the *E. coli* cytochrome *bo*. Kinetic analysis was carried out in the absence of inhibitors (○) and the presence of 0.75 μM LL-Z1272β (▼), 0.2 μM LL-Z1272γ (●), 0.75 μM LL-Z1272δ (▲), and ζ (▽). Data were analyzed based on the Michaelis–Menten kinetics. The apparent K_m and V_{max} values obtained are 23±2 and 1035±28 (control), 43±4 and 841±30 (0.75 μM LL-Z1272β), 64±2 and 402±4 (0.2 μM LL-Z1272γ), 66±3 and 361±6 (0.75 μM LL-Z1272δ), 46±4 μM and 486±14 Q_1H_2/enzyme/s (0.75 μM LL-Z1272ζ), respectively. *R* values were >0.997.